國立臺灣大學生物資源暨農學院動物科學技術學系
碩士論文
Department of Animal Science and Technology
College of Bioresources and Agriculture
National Taiwan University
Master Thesis

丁酸鈉對脂肪細胞分化之調控
The function of sodium butyrate in regulating adipogenesis

鄭穎鴻
Ying-Hung Cheng

指導教授：丁詩同 博士
Advisor: Shih-Torng Ding, Ph.D.

中華民國 104 年 8 月
August, 2015

謝辭

You can't connect the dots looking forward; you can only connect them looking backwards. So you have to trust that the dots will somehow connect in your future. You have to trust in something - your gut, destiny, life, karma, whatever. This approach has never let me down, and it has made all the difference in my life.

- Steve Jobs

這本論文謹獻予伴我完成碩士學位的家人、師長與朋友們。在臺大的兩年間感謝丁詩同老師於學術教導我科學和邏輯思考，使我得以產出論文，於生活也帶給我許多思想上的衝擊，使我能以更成熟的思維待人接物。今日論文能有更佳完整的架構與內容除了丁老師外也要感謝陳洵一老師、陳珠亮老師以及許炯偉老師，諸位老師精闢的見解與建議大大提升論文的完整性，也讓我再次了解科學的深奧。

能在分生室學習科學總讓我倍感幸運，相對充足的資源、儀器設備完善與多元的研究主題，都讓我能更無拘束的構思我的研究，其中特別感謝郁仁學長及原佑學長的循循善誘與提攜，總是無私地傳授實驗技術，認真地與我討論研究和分享人生經驗，今日能以碩士身份踏出臺大，他們有莫大的功勞；另外也感謝虹玟學姊、涵臻學姊和玉惠學姊等認真維持研究室的行政和實驗事宜，使研究室能保有正常的運行，使我能在實驗期間無需分心處理；也感謝裕如學姊、晁偉學長及孟詞學姊等時常為我的實驗提出不同觀點的問題和解決問題之道，有時都能成為我迷失時的一盞明燈；和漋、懿姍等晚輩們在在提醒我必須將所學內化，因為知識並非一味吸收，表達與傳承同樣重要，感謝他們；奪去生命讓我更加珍惜生命，

實驗小鼠、小豬們原諒我無法將你們的生命昇華。

琇慧和禹杉，我總慶幸在研究室有妳們能夠互相勉勵、幫助與分擔，謝謝這兩年的陪伴，願我們未來能夠再遇到如同彼此優質的同伴。

舜堯、俞瑾、偉庭、彥合、志偉、政哲、昱愷、沛嬉和琇涵，比起大學那段歡樂的時光，研究所的艱苦讓我深刻感受到我們這段感情的重要性，人說：『快樂會成雙，痛苦會減半』，謝謝你們讓我感受到這已知的事實。

爸、媽、阿姊和穎駿，感謝你們讓我的溫室期能夠再多幾年，我能很確定告訴你們我得到的絕對不只一張紙，這兩年的累積我更加喜歡我自己，我也會更期待未來的自己能夠達到更高的成就，希望你們以我為榮。

穎鴻 謹識

于國立臺灣大學

中華民國 104 年 8 月

中文摘要

游離短鏈脂肪酸為微生物於腸道發酵後的主要產物，包含乙酸、丙酸、丁酸和戊酸，此類脂肪酸除了提供能量外也會影響腸道上皮細胞黏膜和菌相的生長，除此之外也具有調控免疫系統、癌細胞生長、胰臟分泌胰島素以及細胞分化的作用。目前已有許多研究指出丁酸能夠對脂肪細胞的分化有所作用，而其效果卻不一致，因此本研究的目在釐清丁酸對小鼠、豬等脂肪細胞分化的影響，期能瞭解其作用途徑和機制。我們發現丁酸會抑制小鼠基質血管細胞 (SVCs) 分化成成熟的脂肪細胞，減少脂肪堆積於脂肪細胞中，也會抑制脂肪細胞標的基因表現，包含 *Adipoq* (adiponectin)、*Glut4* (glucose transporter type 4)、*Fasn* (fatty acid synthase)、*Fabp4* (fatty acid binding protein 4) 和 *Srebf1* (sterol regulatory element-binding transcription factor 1) 等，但卻對 3T3-L1 細胞株的分化沒有明顯的影響。相反的，我們發現丁酸會促進豬基質血管細胞分化脂肪細胞，並且會增進脂肪細胞標的基因的表現，包含 *Adipoq*、*Fabp4* 以及 *Cebpa* (CCAAT/enhancer binding protein, alpha) 等，而增加細胞累積油滴。我們進一步探討丁酸對脂肪細胞分化的作用途徑，在小鼠 SVCs 分化過程中額外添加對游離脂肪酸二型受體 (FFAR2) 具有專一性的配體 (4-chloro-α-(1-methylethyl)-N-2-thiazolylbenzeneacetamide, 4-CMTB) ，發現 4-CMTB 也會減少小鼠基質血管細胞的分化，qPCR 分析也顯示脂肪細胞標的基因有下降的情形。綜合上述結果，丁酸對不同物種的脂肪細胞有不一樣的效果，在小鼠中丁酸可能藉由游離脂肪酸二型受體這個路徑來抑制脂肪細胞的分化過程。

關鍵字：丁酸、游離脂肪酸二型受體、脂肪細胞分化、基質血管細胞、小鼠、豬

Abstract

Butyric acid, a short-chain fatty acid (SCFA), is one of the main products from microbial fermentation in the gastrointestinal tract. Free fatty acid receptor 2 (FFAR2) and FFAR3 were found to be receptors for SCFA. In recent years, SCFAs have been shown to play an important role in the prevention and regulation of the metabolic syndrome, certain types of cancer and bowel disorders. Although, the functions of butyrate on adipogenesis were investigated, the results were not consistent. Therefore, we designed the current study to clarify the effects of butyrate on adipocyte differentiation. In the current study, stromal vascular cells (SVC) from murine and porcine subcutaneous adipose tissue (SAT) were used as the preadipocyte model. Adipocyte differentiation degree was assessed by Oil Red O staining and mRNA expression analysis of adipogenic genes. In addition to SVC of mouse and porcine SAT, we also used 3T3-L1 cell line as an *in vitro* model. 4-CMTB, an agonist of FFAR2, was used to determine whether the effects of butyrate are mediated through FFAR2. Compared with control, butyrate inhibited the differentiation of mouse adipocytes. The mRNA expression of adipogenesis related genes, *Adipoq* (adiponectin), *Glut4* (glucose transporter type 4), *Fasn* (fatty acid synthase), *Fabp4* (fatty acid binding protein 4), and *Srebf1* (sterol regulatory element-binding transcription factor 1), were inhibited in mouse adipocytes. In porcine adipocytes, butyrate enhanced the expression of adipogenic genes. On the other hand, 3T3-L1 cell differentiation was not affected by butyrate. 4-CMTB decreased the formation of adipocytes in mouse SVC and the expression of *Adipoq*, *Fabp4* and *Cebpa* (CCAAT/enhancer binding protein, alpha).

Our research demonstrated that butyrate inhibited mouse adipogenesis but enhanced adipogenesis in porcine SVC. Furthermore, the effect of butyrate on adipogenesis may be through the FFAR2 pathway. Further research is required to demonstrate the function of butyrate and the involvement of FFAR2 in regulating human adipogenesis. Such information can support whether murine or porcine model can be used as a better human model in coping with obesity.

Keywords: butyrate, free fatty acid receptor 2, adipogenesis, stromal vascular cell, mouse , porcine

Contents

List of figures

List of tables

1. Introduction

Butyric acid is one of short-chain fatty acids (SCFAs) that are generated physiologically by anaerobic microbial fermentation of dietary fibers in the gastrointestinal tract (Bugaut and Bentéjac, 1993). Major SCFAs contain acetic acid, propionic acid, and butyric acid. SCFAs offer an important energy source for animals, providing ~10-25% of total energy requirement for monogastric animals, and ~60-70% for ruminants (Bergman, 1990). Besides, SCFAs not only benefit the colonic mucosa and intestinal epithelial cells, but also play an important role in colonic homeostasis (den Besten *et al*., 2013). Colonocytes utilize SCFAs as their primary energy source, and they tend to undergo apoptosis easily when there is no SCFA available (Hamer *et al*., 2008). There are four carbons in the molecule of butyric acid ($CH_3CH_2CH_2COO$-H), and butyric acid becomes sodium butyrate (NaB, $CH_3CH_2CH_2COO$-Na) after receiving sodium. NaB is a sodium salt of butyrate used for research experiments because it has the same physiologic function as butyric acid. Moreover, it is much stable than butyric acid. NaB is a natural nutrient and dietary component existed in milk products. It is also produced in a large quantity (from 40 to 100 mM) (den Besten *et al*., 2013), and generated together with other SCFAs from nondigestible carbohydrates, such as

resistant starch, nonstarch polysaccharides, and other low-digestible saccharides (Pryde *et al*., 2002).

In addition to serve as an energy resource, butyric acid or sodium butyrate is also to mediate several physiological functions. Numerous studies suggested that butyrate plays a role in rumen development, gastrointestinal motility, insulin and glucagon secretion, gastrointestinal blood flow, epithelial cell proliferation, cell differentiation, and apoptosis (Bergman, 1990). Recent studies also revealed that dietary supplementation of sodium butyrate can prevent diet-induced obesity and decrease the occurring rate of insulin resistance in mouse models of obesity (Gao *et al*., 2009). Sodium butyrate has also been shown to alleviate metabolic impairments, with overtly functions in anti-obesity and maintaining β-cell function in pregnant obese mouse (Li *et al*., 2013). Butyrate is likely influence insulin sensitivity by stimulating the excretion of gastric inhibitory polypeptide (GIP) and incretin, a glucagon-like peptide 1 (GLP-1), and affect the intestinal barrier function by stimulating the release of GLP-2 (Brahe *et al*., 2013).

In addition, the biofunction for butyrate in the development of colon cancer has been supported by the downregulation of butyrate transporters (*SLC5A8*, a tumor

suppressor gene silenced by methylation) in human colon tumor tissues, which results in a reduced intake and metabolism of butyrate in the colonocytes (Li *et al*., 2003). Butyrate not only has an anti-cacinogenic property, but processes the anti-inflammatory potential in intestinal mucosa (Hamer *et al*., 2008). Butyrate regulates different cells during immune and inflammatory response. It presents multiple effects on migration of leukocytes, production of inflammatory mediators and inducing apoptosis in lymphocytes (Vinolo *et al*., 2011). NF-κB (nuclear factor kappa-light-chain-enhancer of activated B cells), a transcription factor that has an important role in regulating immune response to infection, and IκBα (nuclear factor of kappa light polypeptide gene enhancer in B-cells inhibitor, alpha) is a cellular protein that functions to bind and inhibit the NF-κB (Jacobs and Harrison, 1998). The potential anti-inflammatory mechanism of butyrate is mediated by preventing the degradation of IκBα, and thereby blocked the ability of NF-κB (Yin *et al*., 2001). Furthermore, suppression of NF-κB activation, which may also result from the inhibition of histone deacetylase (HDAC), is the most frequently reported anti-inflammatory function of butyrate (Andoh *et al*., 1999; Yin *et al*., 2001).

Up to sixteen HDACs of human and yeasts were classified into three categories. Class I HDACs are expressed ubiquitously, and with four variances, HDAC1, 2, 3, and 8. Class II HDACs are abundantly expressed in brain, heart, and skeletal muscle, consisting with HDAC4, 5, 6, 7, 9, and 10. Class III HDACs belong to the sirtuin family of HDACs. Besides, HDAC11, a new member of the HDAC family, has also been identified (Gao *et al*., 2002; de Ruijter *et al*., 2003). Biochemically, butyrate can act as a class I HDACs selective inhibitor, and is an necessary agent to inhibit chromatin-remodeling activity by affecting gene expressions and arresting cell proliferation (Davie, 2003). Considering the effect of butyrate on inhibiting HDAC activity and diminishing condensation of the chromatin structure, it is surprising to learn that only 2% of the mammalian gene expression is affected when HDAC activity is inhibited (Davie, 2003). Nevertheless, butyrate is still an effective fatty acid in repressing or stimulating the specific gene expression (Yang *et al*., 2001). Besides butyrate, it has been reported that treatment with other HDAC inhibitors such as trichostatin A (TSA) and suberoylanilide hydroxamic acid (SAHA) induced either cell cycle arrest or cell death, resisted cellular invasion and inhibited angiogenesis leading to a reversed transformation of phenotypes of cancer cells (Xu *et al*., 2007). Many studies

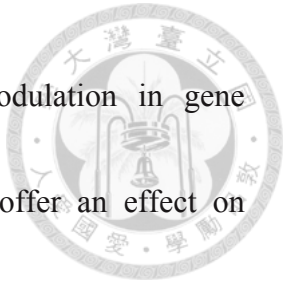

have suggested that HDAC inhibitors, in addition to their modulation in gene expression, inflammatory responses, and anticancer effects, also offer an effect on differentiation of normal cells. Culture with HDAC inhibitors suppressed osteoclast-like cells formation (Rahman *et al*., 2003), induced to pancreatic and hepatic cell differentiation (Haumaitre *et al*., 2008; Henkens *et al*., 2007), accelerated intestine epithelial differentiation (Tou *et al*., 2004), and also regulated myogenesis (McKinsey *et al*., 2001). Additionally, HDAC inhibitors have been demonstrated to modulate adipogenesis, whereas the role of HDACs during adipocyte differentiation is somewhat contentious. For example, several teams demonstrated that HDAC inhibitors from nature sources like TSA or others synthetically developed inhibitors such as valproic acid (VPA), MS-275, and suberoylanilide hydroxamic acid (SAHA) suppressed adipose conversion and adipogenic gene expressions in human preadipocytes or mouse 3T3-L1 cells (Burton *et al*., 2004; Catalioto *et al*., 2009; Kim *et al*., 2009; Lagace and Nachtigal, 2004). In contrast, other groups showed that butyrate can activate transcription factor expressions related to adipogenesis and thus stimulate adipocyte differentiation by reducing HDAC activity in porcine preadipocytes or mouse 3T3-L1 cells (Li *et al*., 2014; Yoo *et al*., 2006). These notions revealed that different kinds of HDAC inhibitors

may influence adipogenesis by suppressing distinct HDACs, or alterative mechanisms that butyrate may go through to regulated adipogenesis.

G protein-coupled receptors (GPRs), also called serpentine receptors, heptahelical receptors, and G protein-linked receptors (GPLR), represents a largest protein family of receptors (Trzaskowski *et al*., 2012). GPRs are also known as seven-transmembrane (7TM) domains. These receptors can sense extremely diverse physiological ligands outside the cell such as amines, amino acids, peptides, proteins, glycoproteins, fatty acids, lipids, phospholipids, steroids, nucleotides hormones, pheromones, ions, odors, and photons (Yonezawa *et al*., 2013). With these various ligands, GPRs transduce extracellular signals across the cell membrane, activate heterotrimeric G proteins and then trigger the second messenger cascades such as the cAMP-dependent protein kinase A and C signaling pathways (Trzaskowski *et al*., 2012; Bindels *et al*., 2013). Lately, a number of orphan GPRs were shown to combine extracellular free fatty acids including SCFAs, middle-chain fatty acids (MCFAs) and long-chain fatty acids (LCFAs), and thus they were renamed as free fatty acid receptor (FFAR) (Brown *et al*., 2003; Le Poul *et al*., 2003; Talukdar *et al*., 2011; Wang *et al*., 2006). FFAR1 (GPR40) is predominantly expressed in the pancreatic β-cells responding to MCFAs and LCFAs

and plays a pivotal role in the enhancement of glucose stimulated insulin secretion (Yonezawa *et al*., 2013). GPR120 (FFAR4) is also activated by MCFAs and LCFAs and related with LCFAs-induced glucagon-like peptide-1 (GLP-1) secretion, increasing insulin sensitivity as well as repression of macrophage-induced inflammation. FFAR1 and GPR120 preferentially bind to LCFAs as compared to MCFAs (Bindels *et al*., 2013; Talukdar *et al*., 2011). Unlike FFAR1 and GPR120, GPR84 is selectively bound to MCFAs only (Wang *et al*., 2006). GPR84 is mainly expressed in bone marrow and several kinds of leukocytes and monocytes, suggesting a role to mediate the functions of free fatty acids on immune system (Blad *et al*., 2012). In contrast to FFAR1, GPR120 and GPR84, FFA2 (GPR43) and FFA3 (GPR41) are activated by SCFAs (Ulven, 2012).

In 2003, two different groups simultaneously identified that formate, acetate, propionate, butyrate, isobutyrate, and pentanoate are all ligand of FFAR3 and FFAR2 (Brown *et al*., 2003; Le Poul *et al*., 2003). They also reported that FFAR3 is related to FFAR2 (52% similarity; 43% identity) and both of them are coupled with $G_{\alpha\, i/o}$ family proteins. Action of FFAR3 and 2 with $G_{\alpha\, i/o}$ results in an increase of intracellular Ca^{2+} concentration and inhibition of the adenylate cyclase pathway. Whereas only FFAR2 couples to $G_{\alpha\, q/11}$ family proteins, and thus activation of FFAR2 with $G_{\alpha\, q/11}$ causes to

stimulation of the phospholipase C (PLC) pathway and raises of intracellular Ca^{2+} levels (Milligan *et al*., 2009). Although FFAR3 and FFAR2 are activated by SCFAs, they have different specificities for carbon chain length. SCFAs bind to FFAR3 in the following order of potency: propionate = butyrate = pentanoate > acetate = formate, while acetate and propionate are the most selective and efficacious ligands for FFAR2 (acetate = propionate > butyrate > pentanoate = formate) (Milligan *et al*., 2009). Current studies, mainly in humans and rodents, have reported that FFAR2 and FFAR3 are expressed in intestine, spleen, and immune tissues, and both receptors mediate the function of SCFAs. For example, FFAR2 and FFAR3 promote inflammatory response in mouse model (Frost *et al*., 2014; Tazoe *et al*., 2008; Kim *et al*., 2013; Li *et al*., 2014; Trompette *et al*., 2014). Additionally, FFAR2 and FFAR3 are also detected in pancreatic tissues and adipose tissues, and thus impact on energy metabolites, but FFAR3 mRNA is not detected in mouse adipose tissues (Blad *et al*., 2012; Frost *et al*., 2014; Hong *et al*., 2005). Acetate can stimulate mouse leptin secretion from epididymal adipocytes, and the mechanism is mediated through FFAR2 pathway (Zaibi *et al*., 2010). However, another group demonstrated that SCFAs augment leptin expression in both mouse primary adipose cells and hasmer CHO-K1 cells by activating FFAR3 (Xiong *et*

al., 2004). It is also reported that acetate and propionate increased lipid accumulation and adipocyte differentiation in mouse 3T3-L1 adipocytes by activating FFAR2, but not through FFAR3 (Hong *et al*., 2005). Besides, acetate and propionate also can activate FFAR2 and result in inhibition of lipolysis in mouse models (Ge *et al*., 2008). As for the effect of FFAR2 on obesity and metabolic abnormalities, it still remains unclear. One group suggested that FFAR2-deficient mice are fatter than wild type mice, whereas mice overexpressing FFAR2 specifically in adipose tissue maintained normal body weight and had suppressed adipose accumulation by blocking insulin signaling in adipocytes (Kimura *et al*., 2013). However, the other groups hold a different view, they showed that *Ffar2*-KO mice changed body composition with increased lean body mass and lower body fat mass, and were able to escape from HFD-induced obesity, leading to better insulin secretion as well as an improvement of glucose tolerance (Bjursell *et al*., 2011; Tang *et al*., 2015). Therefore, whether the role of FFAR2 in obesity needs further stidies.

Adipogenesis is a complex process of cell differentiation by which undifferentiated precursor cells become mature adipocytes (Symonds, 2012). *In vitro* studies using mouse 3T3-L1 and 3T3-F442A cell line and primary human and rodent

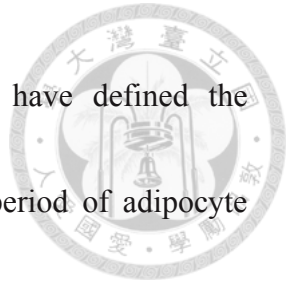

stromal-vascular cells (SVC) isolated from various fat regions have defined the morphological, biochemical and functional changes between the period of adipocyte differentiation (Ntambi and Kim, 2000). When the adipogenic program executes, the transcription factors such as CCAAT/enhancer-binding proteins (CEBPs), peroxisome proliferator-activated receptor gamma (PPARγ), and adipocyte determination and differentiation-dependent factor 1/sterol response element-binding factor 1c (ADD1/SREBF1c) are involved in the cell morphology. The transcriptional cascades also regulate other adipogenic genes giving rise to cell phenotype conversion and accumulation of lipid droplets (Spiegelman *et al*., 1997; Darlington *et al*., 1998; Payne *et al*., 2010). On the other hand, adipose tissue has main role in storing energy in the form of lipid and a major influence on the development of obesity and related complications. Dysregulation of adipose tissue is thought to occupy an important position of many obesity metabolic syndromes (Wang *et al*., 2008). Adipogenetic capability of preadipocytes affects the insulin resistance indeed. Limiting quantities of mature adipocytes in a hypercaloric condition ameliorates the metabolic disease of many organs (Unger *et al*., 2010). For these reasons, a greater understanding of adipogenesis is significant for the healthy metabolism. We previously mentioned that

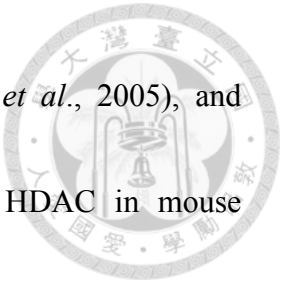

acetate and propionate stimulate adipogenesis via FFAR2 (Hong *et al*., 2005), and butyrate augments adipocyte differentiation by down regulating HDAC in mouse 3T3-L1 cells (Haberland *et al*., 2010; Yoo *et al*., 2006), there are still some conflicting results. Sodium butyrate inhibits mouse mesenchymal stem cells differentiating into adipose cells or fails to influence adipocyte differentiation of primary human preadipocytes (Chatterjee *et al*., 2011; Chen *et al*., 2007). Moreover, there is no study to discuss whether butyrate influences the adipogenesis through FFAR2.

In this study, we observed distinct effects of butyrate on adipocyte differentiation of mouse and porcine SVCs and mouse 3T3-L1 cells. We also found a potential signaling pathway that butyrate may go through to affect adipogenesis in mouse SVC.

2. Materials and Methods

2.1. Isolation of mouse stromal-vascular cells

Mouse stromal-vascular cells (SVCs) isolation followed the previous reported (Aune *et al*., 2013), and all the dissection experiments have been approved by Institutional Animal Care and Use Committee in National Taiwan University. Female mice (7-17 weeks old) were sacrificed, and rinsed with EtOH for sterilizing. Adipose tissues were further removed under sterile conditions from inguinal region of mouse. Approximately, subcutaneous adipose tissues can be harvested about 0.5 g from inguinal region, 3 to 4 mice were pooled for one batch, and tissues were immersed in Dulbecco's Modified Eagle Medium (Invitrogen Life Technologies, Carlsbad, CA). After further clarify like fur or connective tissue from collected sections, inguinal subcutaneous adipose tissues were minced into small pieces, were digested with 1500 U collagenase I/g tissue (Invitrogen Life Technologies, Carlsbad, CA) and 2400 U dispase II/g tissue (Invitrogen Life Technologies, Carlsbad, CA) in 2 ml DMEM in 37˚C for 45-60 min. After digestion, tissues were neutralized with equal volume of complete medium (α-MEM containing 10% FBS and 1% P/S/A). The digested tissues were then filtered with the cell strainer (100 μm diameter). After centrifugation at 700 x g for 10

min at room temperature, oily mature adipocytes (top layer) on the top were be aspirated, and SVC pellets were collected. SVCs pellets were washed with DMEM, mixed well. After centrifugation at 700 x g for 5 min, SVCs pellet was re-suspend in α-MEM, and seeded with appropriate cell density.

2.2. Isolation of porcine stromal-vascular cells

The procedures of cell isolation and culture were conducted as the previously described (Liu *et al*., 2005; Liu *et al*., 2011). Crossbred (LYD) male and female pigs at 7 to 9 days of age were purchased from commercial pig farms. Pigs were killed with electrical stunning coupled with exsanguination, all the animal experiments have been approved by Institutional Animal Care and Use Committee in National Taiwan University. Adipose tissue was removed under sterile conditions from the dorsal subcutaneous depot in the neck, shoulder, and back regions then immersed in DMEM for transportation. Around 40-80 g subcutaneous adipose tissues from the porcine back fat regions were obtained depending on the size of the piglet. Adipose tissues were in 0.66 mm slices in thickness prepared, then minced into small piece. Totally 13 g tissues were digested by 6000 U collagenase (6000 unit/13 g) (Sigma-Aldrich, St. Louis, MO) in 15 mL DMEM at 37˚C for 90 min. After digestion, cells were passed with a single

layer of chiffon. After centrifugation at 800 × g for 10 min at room temperature, the supernatant was discarded and pellet was collected as SVC. SVC pellets were washed three times with DMEM, and further filtered with 70 μm strainer, and cultured in α-MEM with 10% fetal calf serum at a density of 8×10^4 cell/cm^2.

2.3. Sodium butyrate and 4-CMTB treatment

Sodium butyrate (NaB) (Sigma-Aldrich, St. Louis, MO) was dissolved in EtOH for stock, after serious dilution to obtained 5 concentrations: 10, 50, 100, 250, 500 μM, and an equal amount of EtOH was used in control group. About 4-chloro-*α*-(1-methylethyl)-*N*-2-thiazolylbenzeneacetamide (4-CMTB) (Torcris Bioscience, Ellisville, MO) was dissolved in dimethyl sulfoxide (DMSO) (Sigma-Aldrich, St. Louis, MO) for stock. In this study, 4 concentrations: 10^{-2}, 10^{-1}, 1, and 10 μM of 4-CMTB were tested, and identical volume DMSO was added in control group.

2.4. Cell culture and differentiation of mouse and porcine adipocytes

When mouse and porcine SVCs reached confluence (about 3 days after seeding), medium was replaced with differentiation medium [complete culture medium DMEM/F12 with 10 μg/ml insulin, 1 nM 3,3',5-Triiodo-L-thyronine (T3), 10 μg/ml

transferrin (Tf), 0.5 mM 3-isobutyl-1-methylxanthine (IBMX), 1 μM dexamethasone (Dex), and 100 μM indomethacin (IAA) or 100 μM rosiglitazone (RO)] for 3 days to induce adipogenesis. Differentiation medium with IAA was used NaB treatment group, and the other one with RO was for the 4-CMTB treatment group. After 3 days, the differentiation medium was replaced with maintenance medium with the same formula but without Dex, T3, and IAA, or replaced with the maintenance medium with RO. The maintenance medium was replaced every 3 days.

2.5. 3T3-L1 cell culture

3T3-L1 cells (passage number 10-13) were cultured in DMEM with 10% FBS and 1% P/S/A at 37˚C in an atmosphere of 5% CO_2. For adipocyte differentiation, 3T3-L1 cells were cultured with adipogenic differentiation medium (complete culture medium DMEM with 10 μg/ml insulin, 0.5 mM IBMX, and 1 μM Dex). Differentiation medium was replaced every 3 days. Until 9 days for full differentiation.

2.6. Oil Red-O staining

Oil red-O (ORO) staining was used to detect intracellular neutral triglyceride and lipids. 0.5 g ORO (Sigma-Aldrich, St. Louis, MO) was dissolved in 100 ml 100% propylene glycol (Sigma-Aldrich, St. Louis, MO). The ORO solution was filtered with

Whatman #4 filter paper (Whatman International Ltd., Maidstone, England). Cells were washed two times with PBS and incubated with 10% formaldehyde solution for 10 minutes to fix the cells. Formaldehyde solution was discarded and cells were rinsed with tap water three times, then incubated in 100% propylene glycol for 2 minutes. After propylene glycol was removed, ORO solution was added to each well and kept for 30 minutes. After aspirating, plates were washed with 60% propylene glycol for 30 seconds and tap water 5 times. Finally cells were incubated with 10% formaldehyde solution for storage.

2.7. RNA extraction and real-time quantitative PCR analysis

Total RNA was extracted from adipose cells with TRI Reagent (Invitrogen Life Technologies, Carlsbad, CA). RNA samples were digested with DNase I (Ambion, Huntingdon, Great Britain) at 37˚C for 30 minutes to remove genomics DNA and then were reverse transcribed with a High Capacity cDNA Reverse Transcription kit (Applied Biosystems, Foster City, CA). cDNA was amplified by the DyNAmo Flash SYBR Green Kit (Finnzymes, Espoo, Finland), and quantified by an Opticon 2 Real-Time PCR detection System (Bio-Rad, Hercules, CA, USA). The Real-Time PCR program was set as 95˚C for 3 min followed by 40 cycles of 95˚C for 3 seconds, gene-specific annealing

temperature (60˚C) for 20 seconds and then denatured at 95˚C for 10 seconds. The primer sequences for genes measured were listed in Table 1. Primer concentration in the qPCR mixture was 0.1 μM. Amplification of specific transcripts was confirmed by melting curve profile analysis. The 18s and β-actin mRNA were used as the internal control for mouse and porcine model respectively. Relative gene expression was determined by ΔΔCT method. Threshold cycle (Ct) values were obtained and relative gene expression was calculated with the formula $(½)^{\text{Ct target gene} - \text{Ct 18s or β-actin}}$ (Pfaffl, 2001). The PCR amplification efficiency was close to 100%, and all the samples were performed in duplicate.

2.8. Western blot analysis

Mature adipocytes were washed two times with PBS on ice briefly, and homogenized with recommend volume RIPA buffer (Cell Signaling, Beverly, MA). Protein lysates were kept in -80˚C until analysis. Proteins were separated with sodium dodecyl sulfate-10% polyacrylamide gel electrophoresis, and then transferred onto the polyvinylidene fluoride (PVDF) membrane (Perkin Elmer, Waltham, MA, USA) at 400 mA for 90 min in 20% (v/v) methanol, 192 mM glycine and 25 mM Tris/HCL. After transferring, PVDF membrane was blocked with bovine serum albumin (BSA) for 1 hr at

room temperature, washed 3 times with phosphate buffered saline containing 0.1% Treen-20 (PBS/T), and incubated at 4˚C O/N with the primary antibody at 1:1000 dilution for phosphorylated 5' AMP-activated protein kinase pAMPK (Cell Signaling, Beverly, MA), AMPK (Cell Signaling, Beverly, MA) and β-actin (Santa Cruz Biotechnology, Santa Cruz, CA, USA). After washed with PBS/T 3 times, membranes were incubated with proper secondary antibody at 1:10000 dilution at room temperature for 1 hr, and membranes were immersed in the chemiluminescence reagent (Immobilon Western, Millipore, Billerica, Massachusetts, USA) briefly. Membranes then were exposed to the UVP BioSpectrum Imaging System (Upland, CA, USA). Target proteins were quantified by means of the UVP BioSpectrum Imaging System and normalized with the intensity of β-actin in the same sample.

2.9. Statistical analysis

Treatment effects were analyzed with one way ANOVA procedure to determine the major effects of NaB and 4-CMTB. Tukey's test was used to evaluate differences among means (GraphPad Prism 6, Version 6.0c). All data were expressed as mean ± SEM. and P value ≤ 0.05 was considered as statistically significant.

Table 1. Primer used for real-time quantitative PCR analysis

Gene	Sense (5’ 3’)	Antisense (3’ 5’)	Genebank accession number
ADIPOQ	GCTCAGGATGCTGTTGTTGG	TGGTGGAGGCTCTGAGTTGG	NM_214370.1
CEBPα	TCGACATCAGCGCCTACATC	GCCTTGGCCTTCTCTTGCT	XM_003127015.2
FASN	GTGGGCTACAGCATGAATAGG	GAATTGCAGCGAGGAGTTAG	NM_001099930.1
GLUT4	ATGACTGTGGCTCTGCTTCC	CTCGAGTTCTGTGCTGGGTT	NM_001128433.1
LPL	TGGACGGTGACAGGAATGTA	AAGGCTGTATCCCAGGAGGT	NM_008509.2
PPARγ	TCGCATCTTTCAGGGGTGTC	CCCAGGGATGTTCTTGGCAT	NM_214379.1
SREBF1	CCACCAGTCCTGATGCCAG	GTACATCTTCAGCGGGGTGG	NM_001198694.2
β-ACTIN	GCCAGGTCATCACCATCGG	GTAGAGGTCCTTGCGGATGTC	AF054837.1
Adipoq	TGACGACACCAAAGGGCTC	CCAACCTGCACAAGTTCCCT	NM_009605.4
Cebpα	GAAGGTGTTGGAGTTGACCAG	CCGCAGCGTGTCCAGTTCACGG	NM_001287514.1
Cebpβ	GGACTACGCAACACACGTGTAACT	ACAAAACCAAAAACATCAACAAACC	NM_001287738.1
Cebpδ	CCCCGGAGCTCAATGGGGGA	CTTGTCCCCGCACACCCGAC	NM_007679.4
Fabp4	TCACCATCCGGTCAGAGAGT	CCAGCTTGTCACCATCTCGC	NM_024406.2
Fasn	GGGCACTGACTGTCTGTTTTC	GGATCAGGAGAGCATCAAGAG	NM_007988.3
Glut4	TACATACCTGACAGGGCAAGG	TTCGGGTTTAGCACCCTTC	NM_009204.2
Pparγ	GCCTGCGGAAGCCCTTTGGT	AAGCCTGGGCGGTCTCCACT	NM_001127330.2
Srebf1	GCAGACCCTGGTGAGTGGA	GTCGGTGGATGGGCAGTTT	NM_001001144.3
Rn18s	CTTCTCAGCGCTCCGCCAGG	TTGTACACACCGCCCGTCGC	NR_003278.3

3. Results

3.1. Establish the adipocyte differentiation model in mouse and porcine SVCs and 3T3-L1 cell

In this research, we used three kinds of cells, mouse and porcine SVCs and mouse 3T3-L1 cells were used as *in vitro* models. The first step was to confirm 3T3-L1 cells and isolated SVCs differentiation into adipocytes. As shown in figure 1A, figure 2A, and figure 3A, cells with lipid droplets became visible on day 9. Results were also qualified by Oil Red O staining (Figure 1B, 2B, and 3B). Adiponectin (*Adipoq*) is a hormone derived frome mature adipocytes, is a marker of late adipocyte differentiation (Fu *et al*., 2005). Peroxisome proliferator-activated receptor gamma (*Pparγ*) and CCAAT/enhancer-binding protein alpha (*Cebpα*) two transcription factors of adipocytes are known as early adipogenic markers (Ntambi and Kim, 2000; Rosen and MacDougald, 2006). In mouse SVCs model, the mRNA level of *Adipoq* increased from day 2 to day 9 (Figure 4A). The mRNA abundance of *Pparγ* and *Cebpα* significantly increased on day 4 of differentiation as compared with day 2, and then expression level declined to day 9 (Figure 4B and C). These results suggested that SVCs collected in our studies can differentiate into mature adipocytes.

3.2. Effects of sodium butyrate on adipocyte differentiation in mouse SVCs

Figure 1 shoes the mature adipocyte differentiation in mouse SVCs on day 9 by Oil Red O-stained. Results of lipid droplet accumulation indicated that mouse SVCs treated with 50, 100, 250, or 500 μM NaB formed less adipocytes than untreated one. Quantitative analysis of lipid droplet area showed higher concentrations of NaB decreased lipid droplet accumulation in mature mouse adipocytes (Figure 1C). Mouse SVCs had poor differentiation in presence of 500 μM NaB with the lower mRNA leads of adipogenic markers than lower concentrations and control groups (Figure 5A-D). In mouse SVCs, the expression of *Adipoq* was significantly decreased in 250 and 500 μM NaB group as compared to the control (Figure 5A). Expression of fatty acid binding protein 4 (*Fabp4*), glucose transporter type 4 (*Glut4*), and fatty acid synthase (*Fasn*) in 500 μM NaB group were significantly lower than the control (Figure 5B-D).

3.3. Effects of sodium butyrate on transcription factors in mouse SVCs

Adipocyte differentiation is mainly controlled by the transcription factors *Pparγ* and *Cebpα*, and by other factors, such as sterol regulatory element-binding transcription factor 1 (*Srebf1*), CCAAT/enhancer-binding protein beta (*Cebpβ*) and CCAAT/enhancer-binding protein delta (*Cebpδ*) (Ntambi and Kim, 2000). We

elucidated the effects of different does of NaB on expression of *Pparγ*, *Cebpα*, and *Srebf1* in mouse SVCs (Figure 6A-C). Compared with control group, cells treated with 10, 50, 100, 250, 500 μM NaB for 9 days did not alter expression of *Pparγ* and *Cebpα* genes (Figure 6A and B), but *Srebf1* mRNA level as significantly decreased in the 500 μM NaB treated group (Figure 6C). *Cebpα* appears to have diverse roles in differentiation of preadipocyte. After inducton of differentiation, expression of *Cebpβ* and *Cebpδ* in preadipocytes increase rapidly and transiently (Darlington *et al*., 1998). In our study, we treated with different doses of NaB in mouse SCVs, and the expression of *Cebpβ* was significantly decreased in NaB treated group, but *Cebpδ* not (Figure 7A and B). In sum, these results indicated that NaB can inhibit adipocyte differentiation in mouse SVCs.

3.4. Sodium butyrate has no effect on adipocyte differentiation in mouse 3T3-L1 cell line

To comfirm the results from mouse SVCs, we next determined whether NaB can inhibite adipocyte differentiation of mouse 3T3-L1 cells. Neither lipid accumulation (Figure 2A-C) or adipogenic marker mRNA expression detected by qPCR (Figure 8 and Figure 9) was not affected by NaB at various levels. Representative images of Oil Red

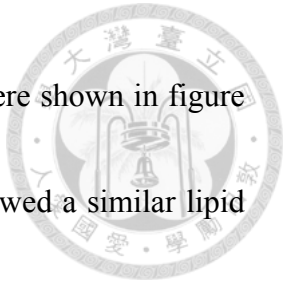

O-stained mouse 3T3-L1 cells at day 9 of induced differentiation were shown in figure 2B. Mature adipocytes treated with different concentration NaB showed a similar lipid droplet formation grade. Compared to control group, *Adipoq*, *Fabp4*, *Fasn*, *Glut4* (Figure 8A-D), *Pparγ*, *Cebpα* and *Srebf1* gene (Figure 9A-C) expression in NaB treated group were not affected by NaB treatment.

3.5. Effects of sodium butyrate on adipocyte differentiation in porcine SVCs

Distinct effects of NaB on adipocyte differentiation between mouse SVCs and mouse 3T3-L1 cells were observed. Since it have been reported that NaB enhances adipocyte differentiation in porcine SVCs (Li *et al*., 2014), the possibilities to cause the distinctive effects were examined including mouse SVCs isolation, differentiation system, and the method of NaB treatment. On the other hand, to obtain the comparison of species difference between mouse and porcine, we treated the porcine SVCs with the sure concentrations of NaB. Along the induced differentiation up to 9 days, lipid accumulation of porcine SVCs treated with 10, 50, 100, 250 or 500 μM NaB increased gradually (Figure 3A and B). Quantitative analysis of these images also indicated a higher degree of differentiation of porcine SVCs in the presence of 500 μM NaB than the control group (Figure 3C). In 500 μM NaB treatment group, porcine SVCs had greater expression for 5

[*FASN*, *LPL* (lipoprotein lipase), *PPARγ*, *CEBPα*, and *SREBF1*] of the seven adipogenic markers than untreated SVCs (Figure 5C and D; Figure 6A-C). These results reconfirmed Li *et al* (2014) suggested that NaB promotes adipocyte differentiation of porcine SVCs. In addition, we offered a circumstantial evidence that our experiment procedure is feasible.

3.6. The effects of 4-CMTB on adipocyte differentiation in mouse SVCS

FFAR2 has been identified as a receptor for SCFAs (Bindels *et al*., 2013; Brown *et al*., 2003; Xiong *et al*., 2004), and FFAR2 was found to regulate the adipogenic effect of acetate and propionate on adipocyte differentiation in mouse 3T3-L1 cells (Hong *et al*., 2005). We therefore asked the question whether NaB affects adipogenic marker expressions and thereby adipocyte differentiation in mouse and porcine SVCs through FFAR2. Therefor we used 4-CMTB, a FFAR2 agonist, to affect adipocyte differentiation (Milligan *et al*., 2009; Smith *et al*., 2011). 4-CMTB binds to different locations from the orthosteric sites, and mimic the activity effects of butyrate on adipogenic marker expressions in mouse SVCs. As observed in figure 12A, B and C, Oil Red O staining of mouse SVCs cultured with 4-CMTB for 9 days showed poor differentiation than those non 4-CMTB treatment group. In the presence of 4-CMTB

mouse SVCs also showed significantly lower expression of adipoenic markers including *Adipoq*, *Fabp4* and *Cebpα* than the control without 4-CMTB (Figure 13A and B; Figure 14B).

3.7. No obvious effects of NaB and 4-CMTB on AMPK activity

AMPK is known to play an important role in regulating glucose and lipid metabolism. Phosphorylation of AMPK induces inhibition of lipolysis, and downregulatation of important adipogenic genes, such as *PPARγ* and *CEBPα* (Dagon *et al*., 2006). To test the possibility that NaB and 4-CMTB inhibites adipocyte differentiation and decreases expression of adipose markers by enhancing the activity of AMPK, we analyzed the phosphorylated level of AMPK. As shown in figure 15A and B, NaB (250 and 500 μM) and 4-CMTB (1 and 10 μM) treatment did not cause a significant change of pAMPK/AMPK ratio respectively (Figure 15A and B).

A

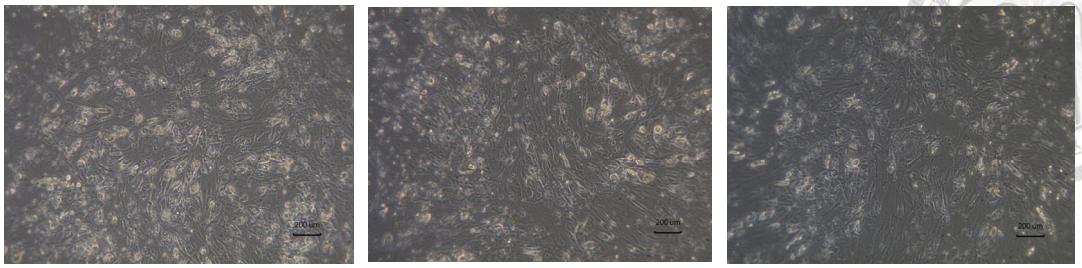

CTRL　　NaB 10 μM　　NaB 50 μM

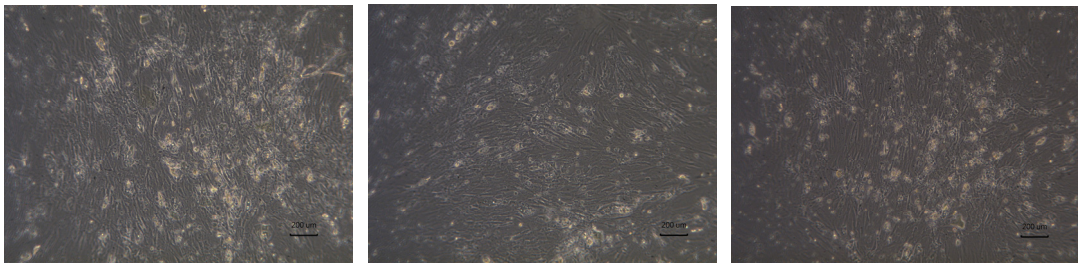

NaB 100 μM　　NaB 250 μM　　NaB 500 μM

B

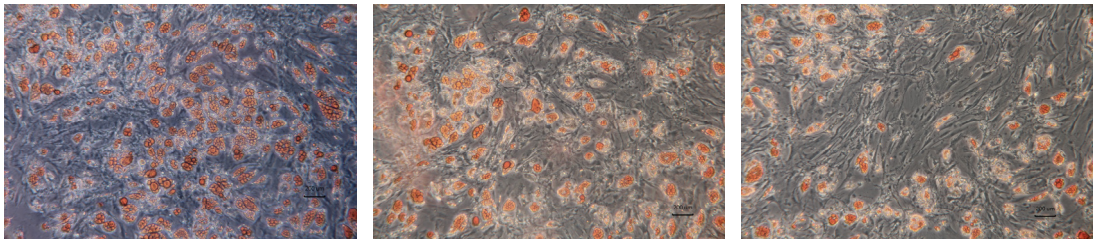

CTRL　　NaB 10 μM　　NaB 50 μM

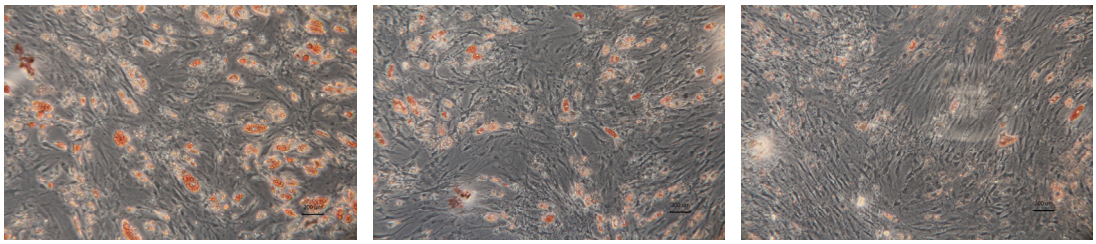

NaB 100 μM　　NaB 250 μM　　NaB 500 μM

C

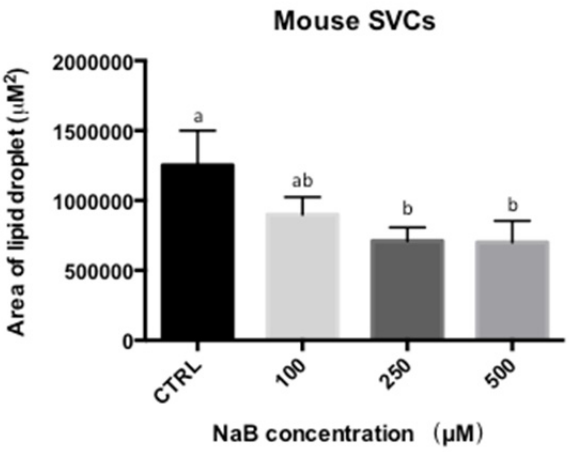

Figure 1. Effects of NaB on adipocyte differentiation in mouse SVCs. Mouse SVCs were induced for differentiation in the presence of 0, 10, 50, 100, 250 or 500 μM NaB for 9 days. (A) Mature adipocytes at day 9 of differentiation (200 x magnification). (B) Representative images of Oil Red O-stained cells (200 x magnification). (C) Quantification of area of mature mouse adipocytes lipid droplets (μM^2). Data are presented as means ± SEMs, different letters indicate statistical significance, n = 3.

A

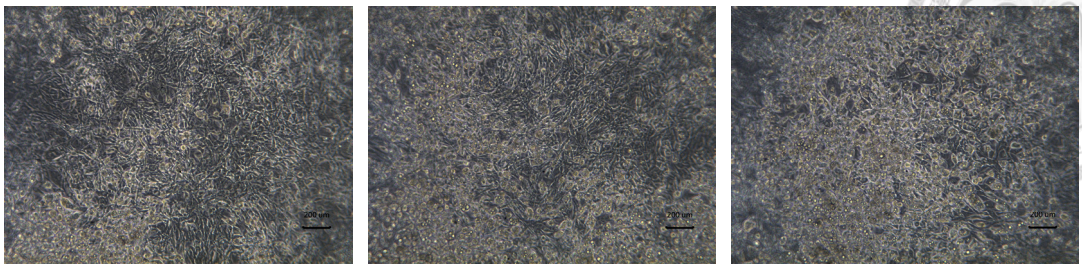

CTRL NaB 10 μM NaB 50 μM

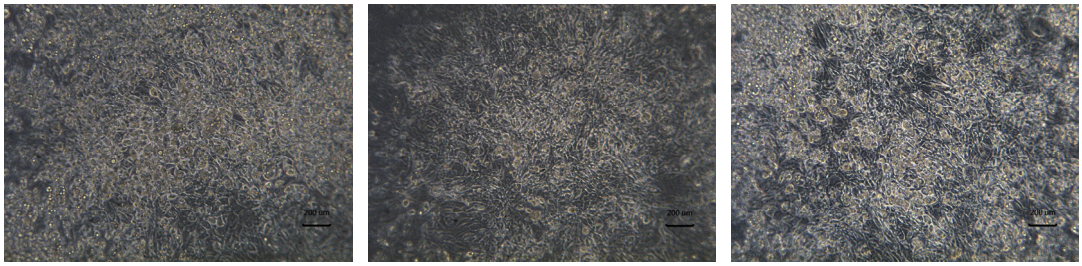

NaB 100 μM NaB 250 μM NaB 500 μM

B

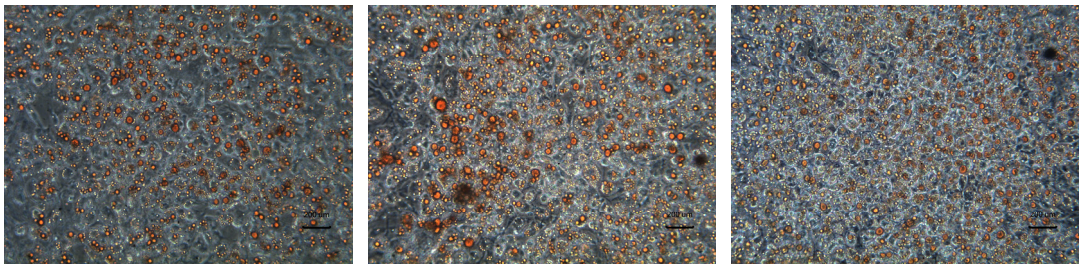

CTRL NaB 10 μM NaB 50 μM

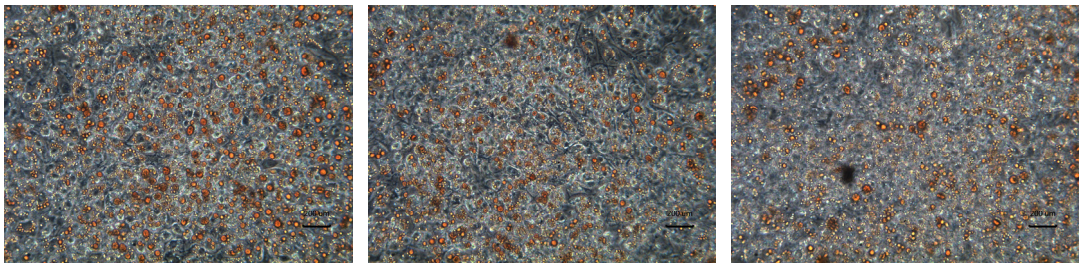

NaB 100 μM NaB 250 μM NaB 500 μM

C

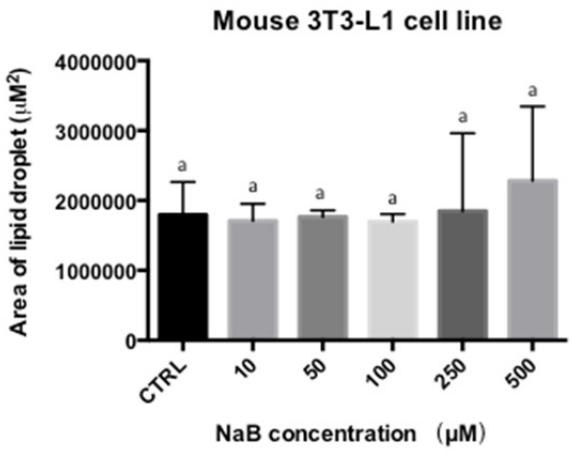

Figure 2. Effects of NaB on adipocyte differentiation in mouse 3T3-L1 cell line. Mouse 3T3-L1 cells were induced for differentiation in the presence of 0, 10, 50, 100, 250 or 500 μM NaB for 9 days. (A) Mature adipocytes at day 9 of differentiation (200 x magnification). (B) Representative images of Oil Red O-stained cells (200 x magnification). (C) Quantification of area of mature mouse 3T3-L1 adipocytes lipid droplets (μM^2). Data are presented as means ± SEMs, different letters indicate statistical significance, n = 3.

A

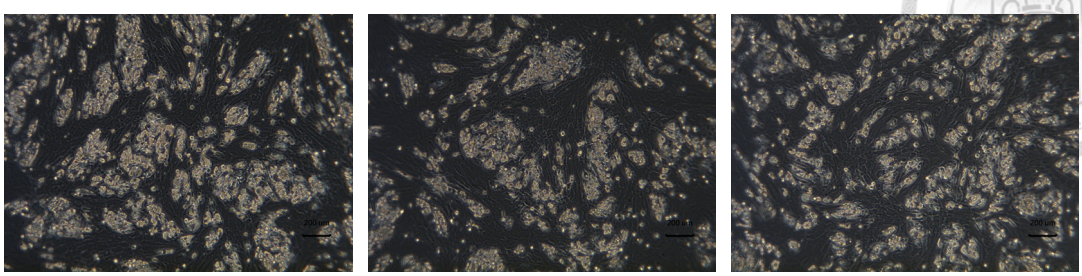

CRTL NaB 10 μM NaB 50 μM

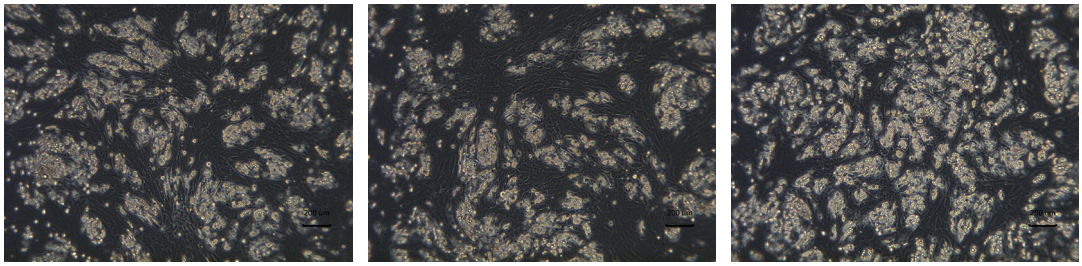

NaB 100 μM NaB 250 μM NaB 500 μM

B

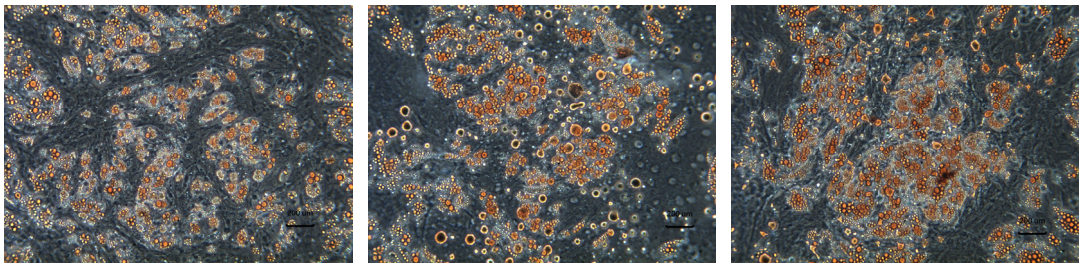

CTRL NaB 10 μM NaB 50 μM

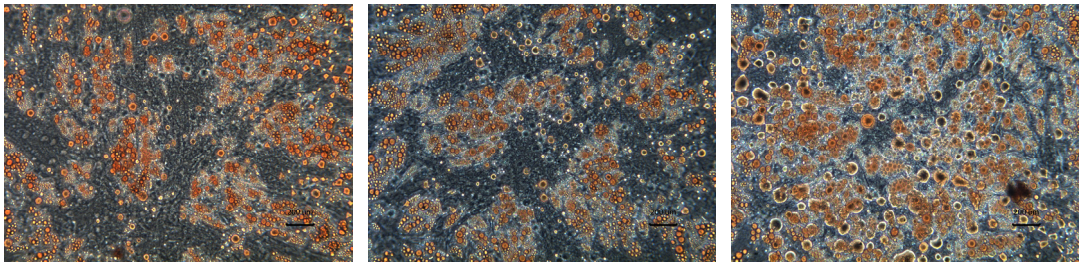

NaB 100 μM NaB 250 μM NaB 500 μM

C

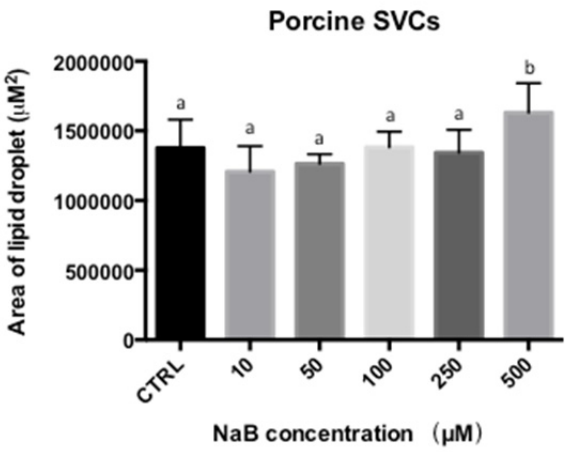

Figure 3. Effects of NaB on adipocyte differentiation in porcine SVCs. Porcine SVCs were induced or differentiation in the presence of 0, 10, 50, 100, 250 or 500 μM NaB for 9 days. (A) Mature adipocytes at day 9 of differentiation (200 x magnification). (B) Representative images of Oil Red O-stained cells (200 x magnification). (C) Quantification analysis of area of mature porcine SVCs adipocytes lipid droplets (μM^2). Data are presented as means ± SEMs, different letters indicate statistical significance, n = 3.

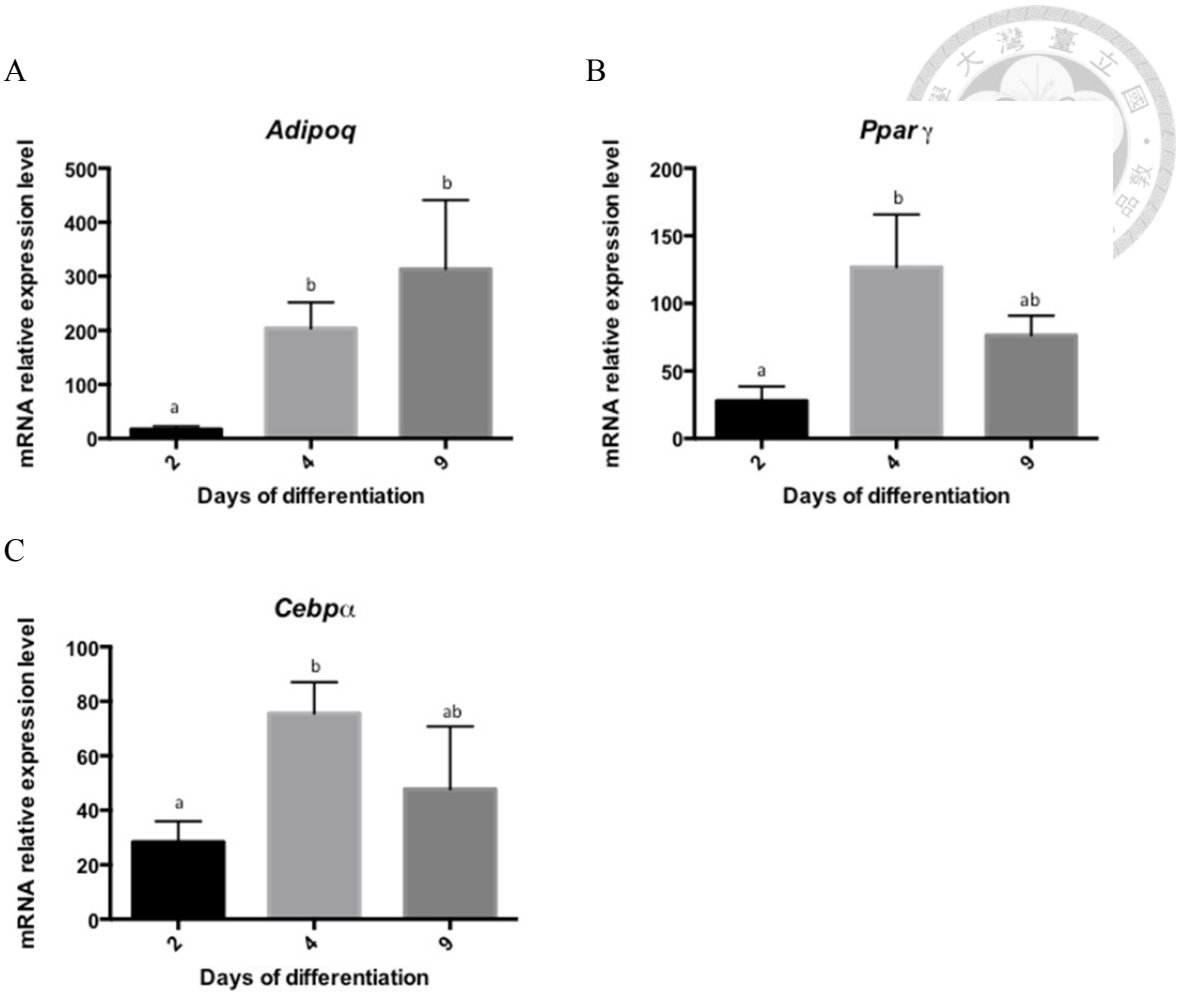

Figure 4. Expression of adipogenic markers of mouse SVCs. Mouse SVCs were induced for differentiation for 9 days. Adipogenic marker expression (A) adiponectin (*Adipoq*), (B) peroxisome proliferator-activated receptor gamma (*Pparγ*), and (C) CCAAT/enhancer-binding protein alpha (*Cebpα*) were analyzed at day 2, 4, and 9. Data were normalized with 18S mRNA, and presented as means ± SEMs, different letters indicate statistical significance, n = 3, a, b, and c indicate significant difference at $P \leq 0.05$.

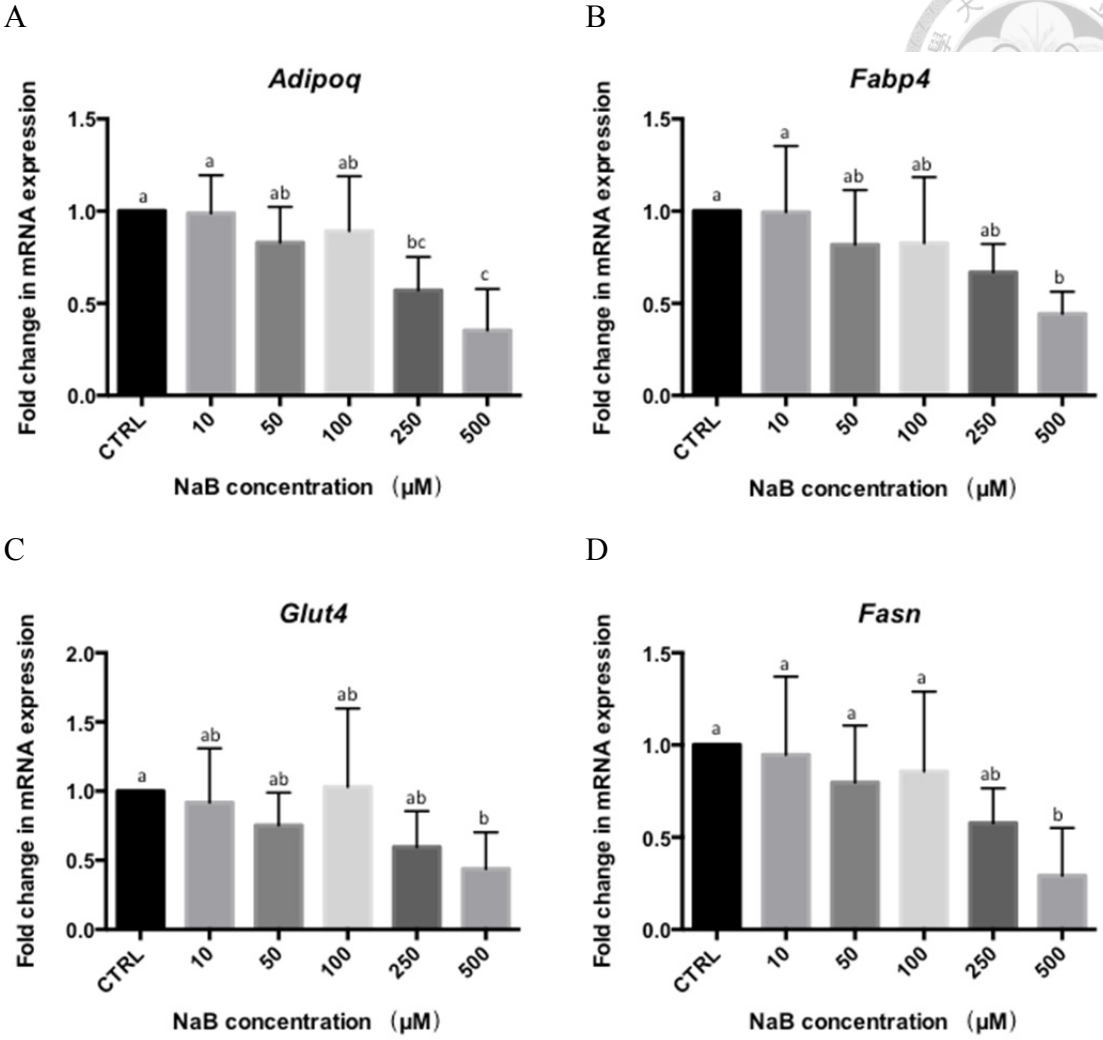

Figure 5. Effects of NaB on adipogemic markers expression in mouse SVCs. Mouse SVCs were induced for differentiation in the presence of 0, 10, 50, 100, 250 or 500 μM NaB or the vehicle EtOH. Relative expression of (A) adiponectin (*Adipoq*), (B) fatty acid binding protein 4 (*Fabp4*), (C) glucose transporter type 4 (*Glut4*), and (D) fatty acid synthase (*Fasn*) genes at day 9 were analyzed by real-time qPCR. Data were normalized with 18S mRNA, and presented as means ± SEMs, different letters indicate statistical significance, n = 7, a, b, and c indicate significant difference at $P \leq 0.05$.

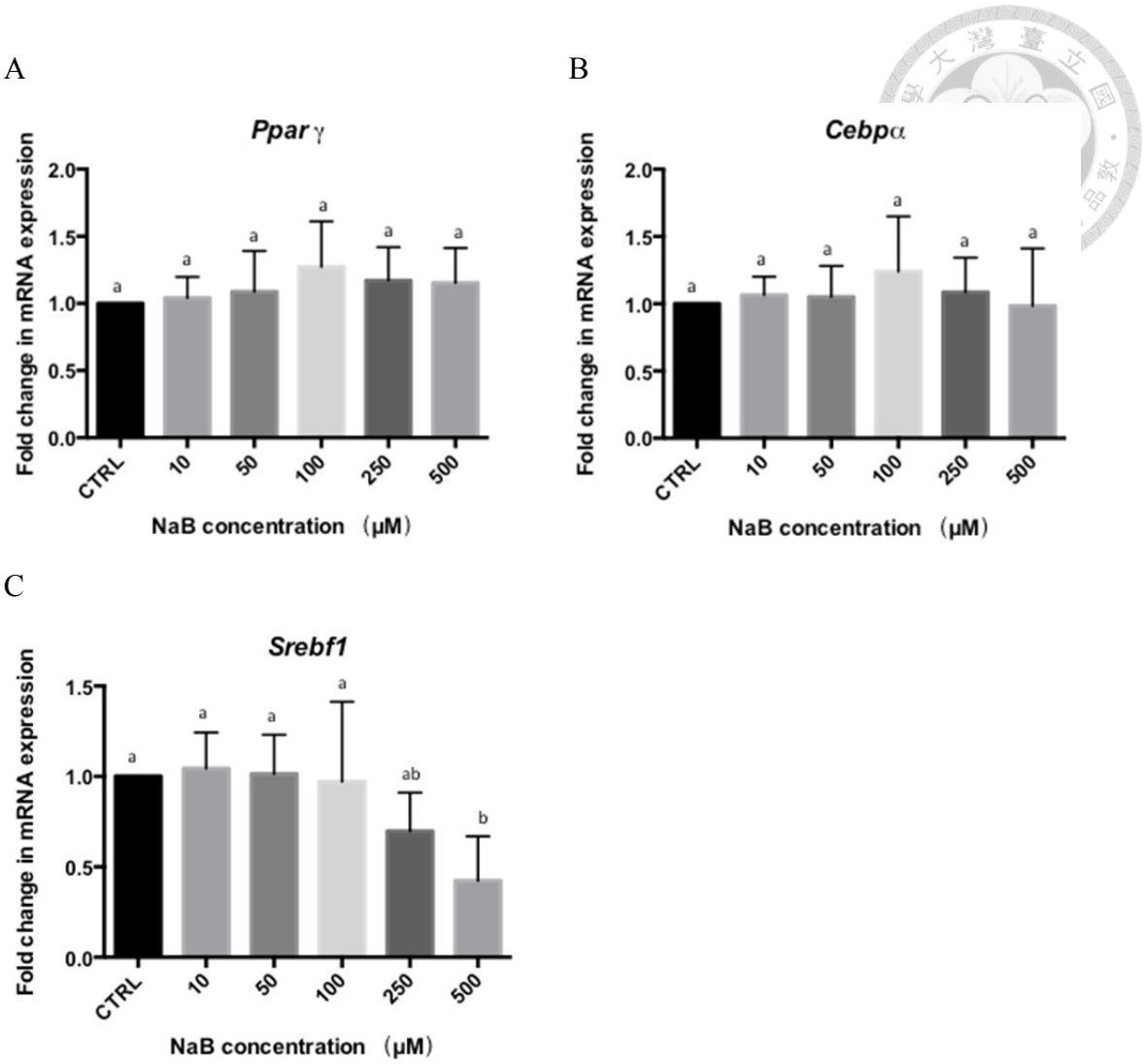

Figure 6. Effects of NaB on transcription factors in mouse SVCs. Mouse SVCs were induced for differentiation in the presence of 0, 10, 50, 100, 250 or 500 μM NaB or the vehicle EtOH. Relative expression of (A) peroxisome proliferator-activated receptor gamma (*Pparγ*), (B) CCAAT/enhancer-binding protein alpha (*Cebpα*), and (C) sterol regulatory element-binding transcription factor 1 (*Srebf1*) genes at day 9 were analyzed by real-time qPCR. Data were normalized with 18S mRNA, and presented as means ± SEMs, different letters indicate statistical significance, n = 7, a, b, and c indicate significant difference at $P \leq 0.05$.

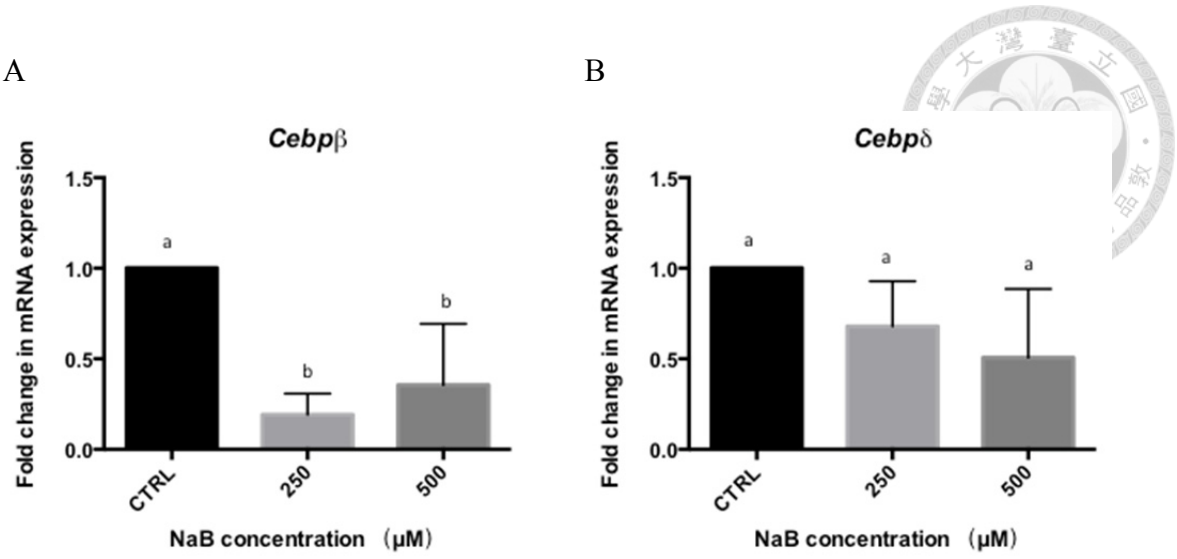

Figure 7. Effects of NaB on transcription factors in mouse SVCs. Mouse SVCs were induced for differentiation in the presence of 0, 250 or 500 μM NaB or the vehicle EtOH. Relative expression of (A) CCAAT/enhancer-binding protein beta (*Cebpβ*) and (B) CCAAT/enhancer-binding protein delta (*Cebpδ*) genes at day 4 were analyzed by real-time qPCR. Data were normalized with 18S mRNA, and presented as means ± SEMs, different letters indicate statistical significance, n = 4, a, b, and c indicate significant difference at $P \leq 0.05$.

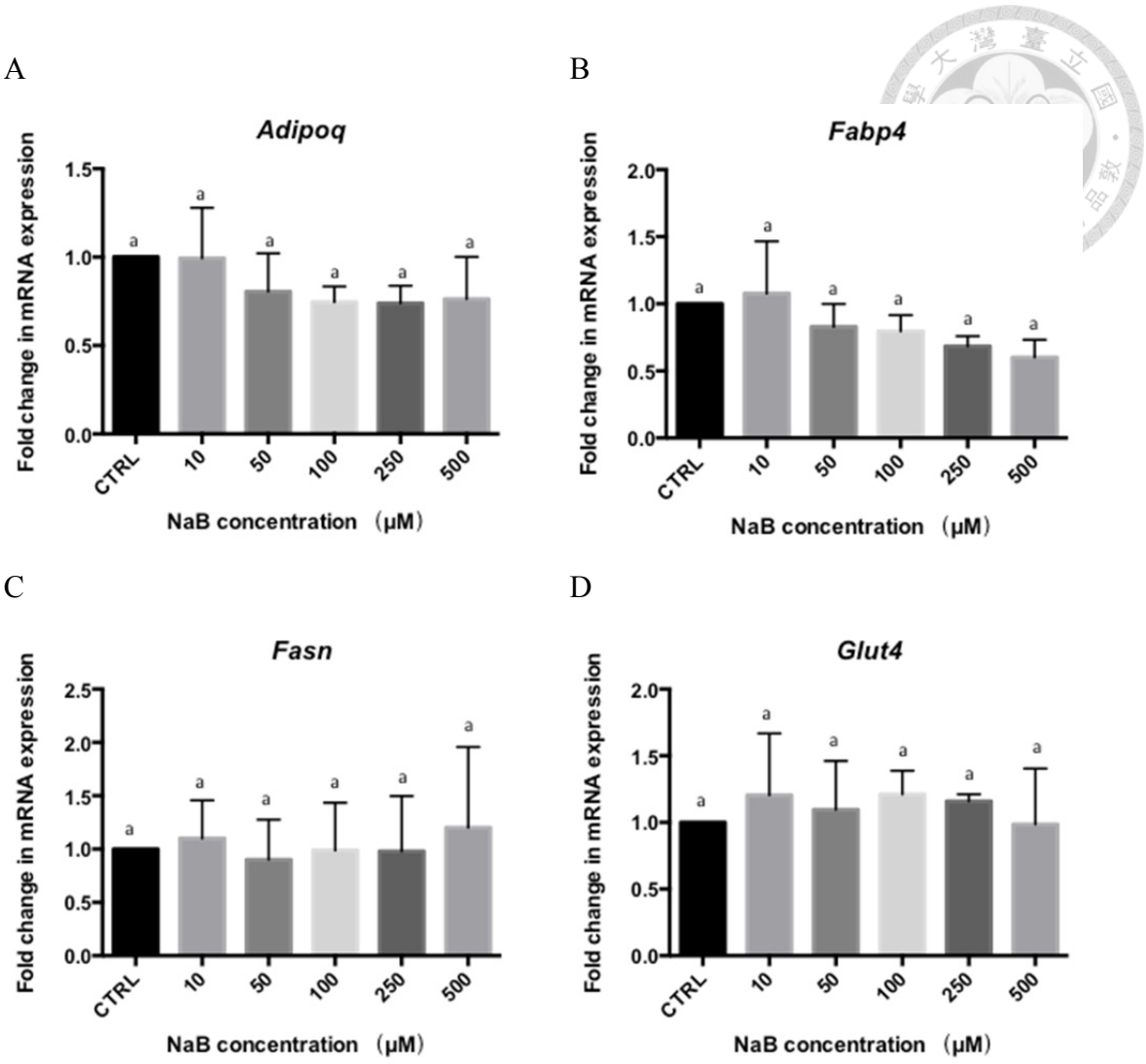

Figure 8. Effects of NaB on adipogenic markers in mouse 3T3-L1 cell line. Mouse 3T3-L1 cell line SVCs were induced for differentiation in the presence of 0, 10, 50, 100, 250 or 500 μM NaB or the vehicle EtOH. Relative mRNA expression of (A) adiponectin (*Adipoq*), (B) fatty acid binding protein 4 (*Fabp4*), (C) glucose transporter type 4 (*Glut4*), and (D) fatty acid synthase (*Fasn*) genes at day 9 were analyzed by real-time qPCR. Data were normalized with 18s mRNA, and presented as means ± SEMs, different letters indicate statistical significance, n = 3, a, b, and c indicate significant difference at $P \leq 0.05$.

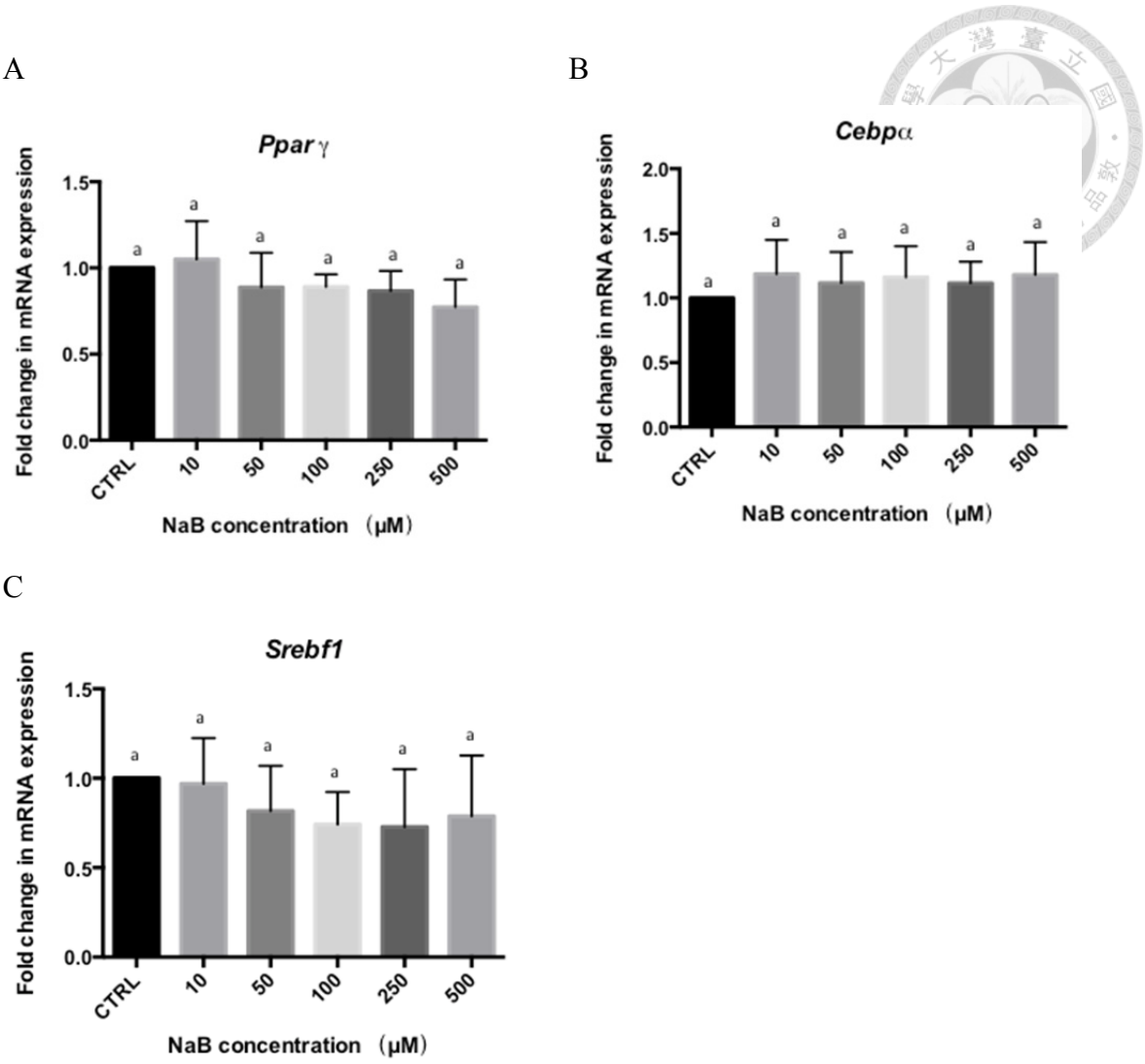

Figure 9. Effects of NaB on transcription factors in mouse 3T3-L1 cell line. Mouse 3T3-L1 cells were induced for differentiation in the presence of 0, 10, 50, 100, 250 or 500 μM NaB or the vehicle EtOH. Relative mRNA expression of (A) peroxisome proliferator-activated receptor gamma (*Pparγ*), (B) CCAAT/enhancer-binding protein alpha (*Cebpα*), and (C) sterol regulatory element-binding transcription factor 1 (*Srebf1*) genes at day 9 were analyzed by real-time qPCR. Data were normalized with 18s mRNA, and presented as means ± SEMs, different letters indicate statistical significance, n = 3, a, b, and c indicate significant difference at $P \leq 0.05$.

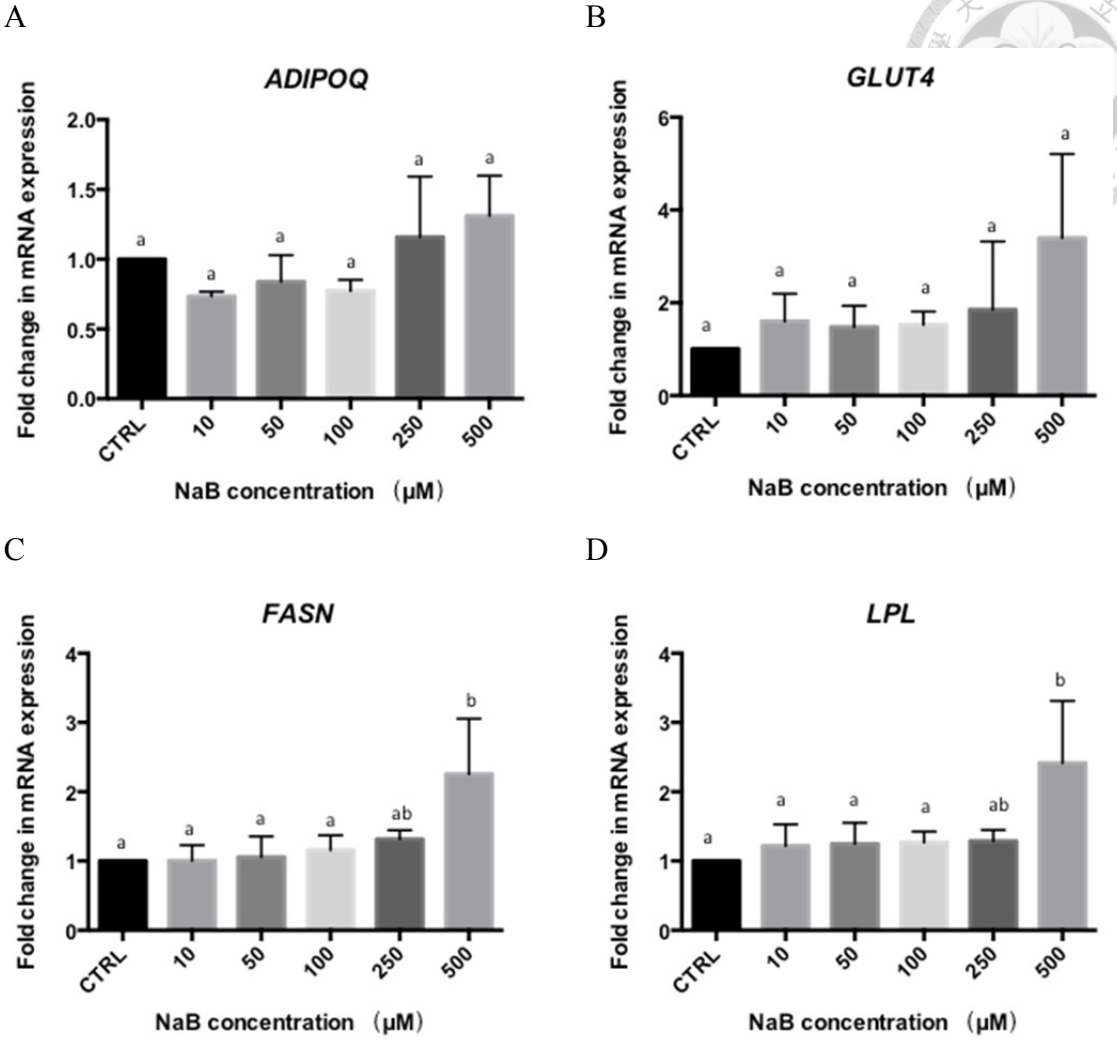

Figure 10. Effects of NaB on adipogenic markers in porcine SVCs. Porcine SVCs were induced for differentiation in the presence of 0, 10, 50, 100, 250 or 500 μM NaB or the vehicle EtOH. Relative mRNA expression of (A) adiponectin (*ADIPOQ*), (B) glucose transporter type 4 (*GLUT4*), (C) fatty acid synthase (*FASN*) mRNAs, and (D) lipoprotein lipase (*LPL*) genes at day 9 were analyzed by real-time qPCR. Data were normalized with *β-ACTIN* mRNA, and presented as means ± SEMs, different letters indicate statistical significance, n = 7, a, b, and c indicate significant difference at $P \leq 0.05$.

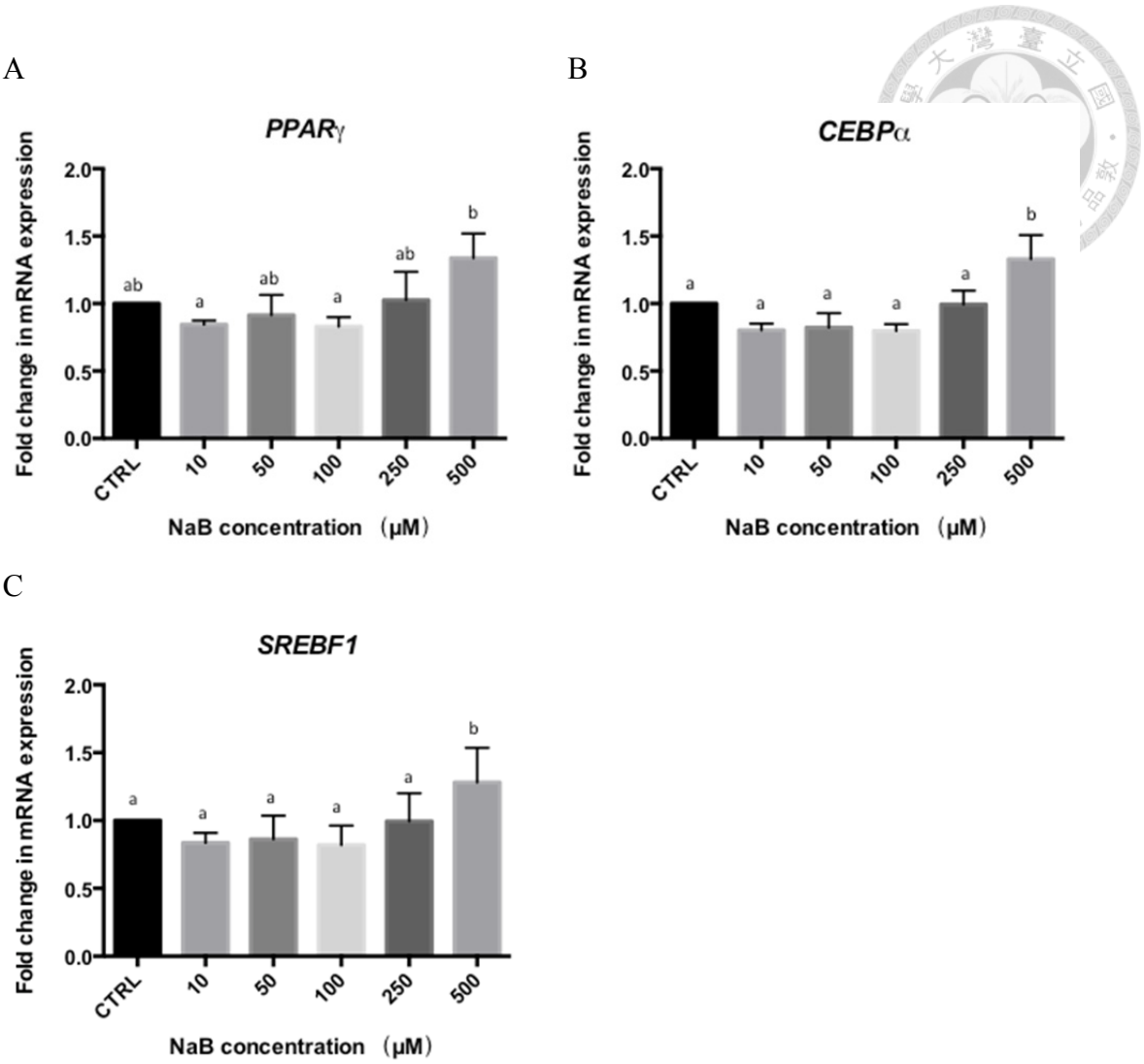

Figure 11. Effects of NaB on transcription factors in porcine SVCs. Porcine SVCs were induced for differentiation in the presence of 0, 10, 50, 100, 250 or 500 μM NaB or the vehicle EtOH. Relative mRNA expression of (A) peroxisome proliferator-activated receptor gamma (*PPARγ*), (B) CCAAT/enhancer-binding protein alpha (CEBPα), and (C) sterol regulatory element-binding transcription factor 1 (*SREBF1*) genes at day 9 were analyzed by real-time qPCR. Data were normalized with *β-ACTIN* mRNA, and presented as means ± SEMs, different letters indicate statistical significance, n = 3, a, b, and c indicate significant difference at $P \leq 0.05$.

A

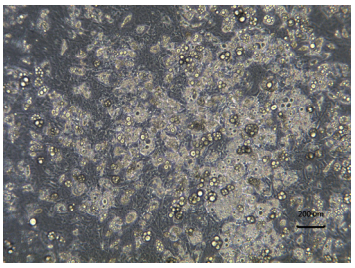

CTRL

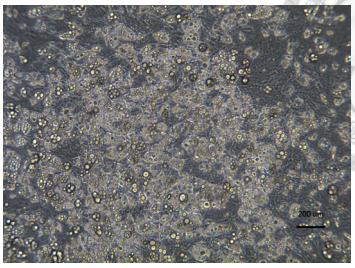

4-CMTB 10^{-2} µM

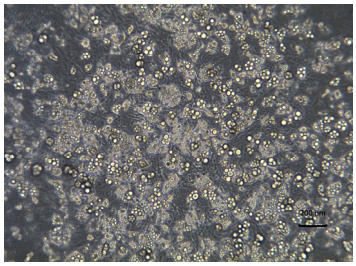

4-CMTB 10^{-1} µM

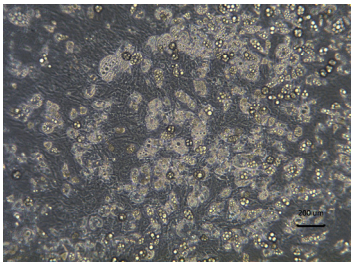

4-CMTB 1 µM

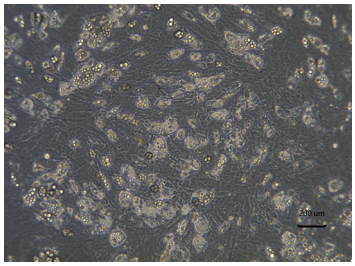

4-CMTB 10 µM

B

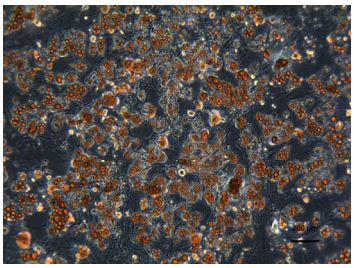

CTRL

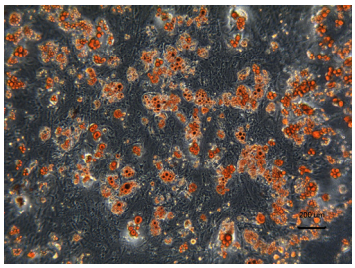

4-CMTB 10^{-2} µM

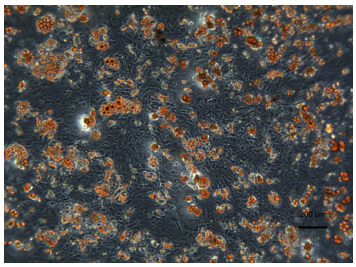

4-CMTB 10^{-1} µM

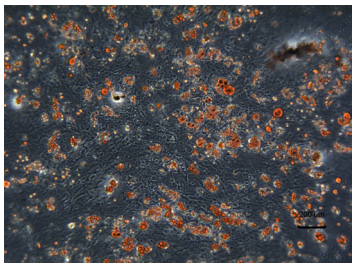

4-CMTB 1 µM

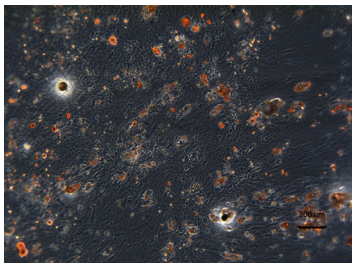

4-CMTB 10 µM

C

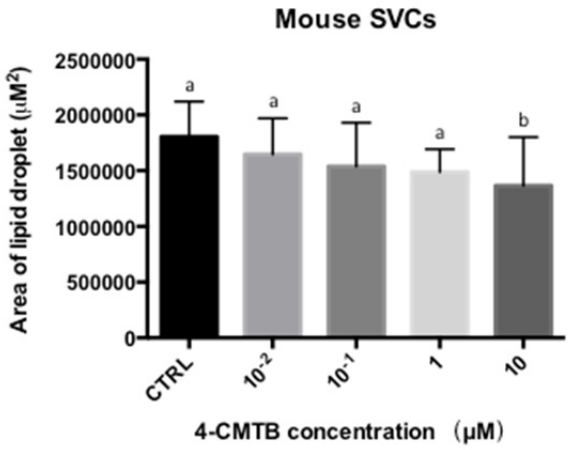

Figure 12. Effects of 4-CMTB on adipocyte differentiation in mouse SVCs. Mouse SVCs were induced for differentiation in the presence of 0, 10^{-2}, 10^{-1}, 1, or 10 μM 4-CMTB for 9 days. (A) Mature adipocytes at day 9 of differentiation (200 x magnification). (B) Representative images of Oil Red O-stained cells (200 x magnification). (C) Area of lipid droplets in mature mouse SVCs adipocytes (μM^2). Data are presented as means ± SEMs, different letters indicate statistical significance, n = 5.

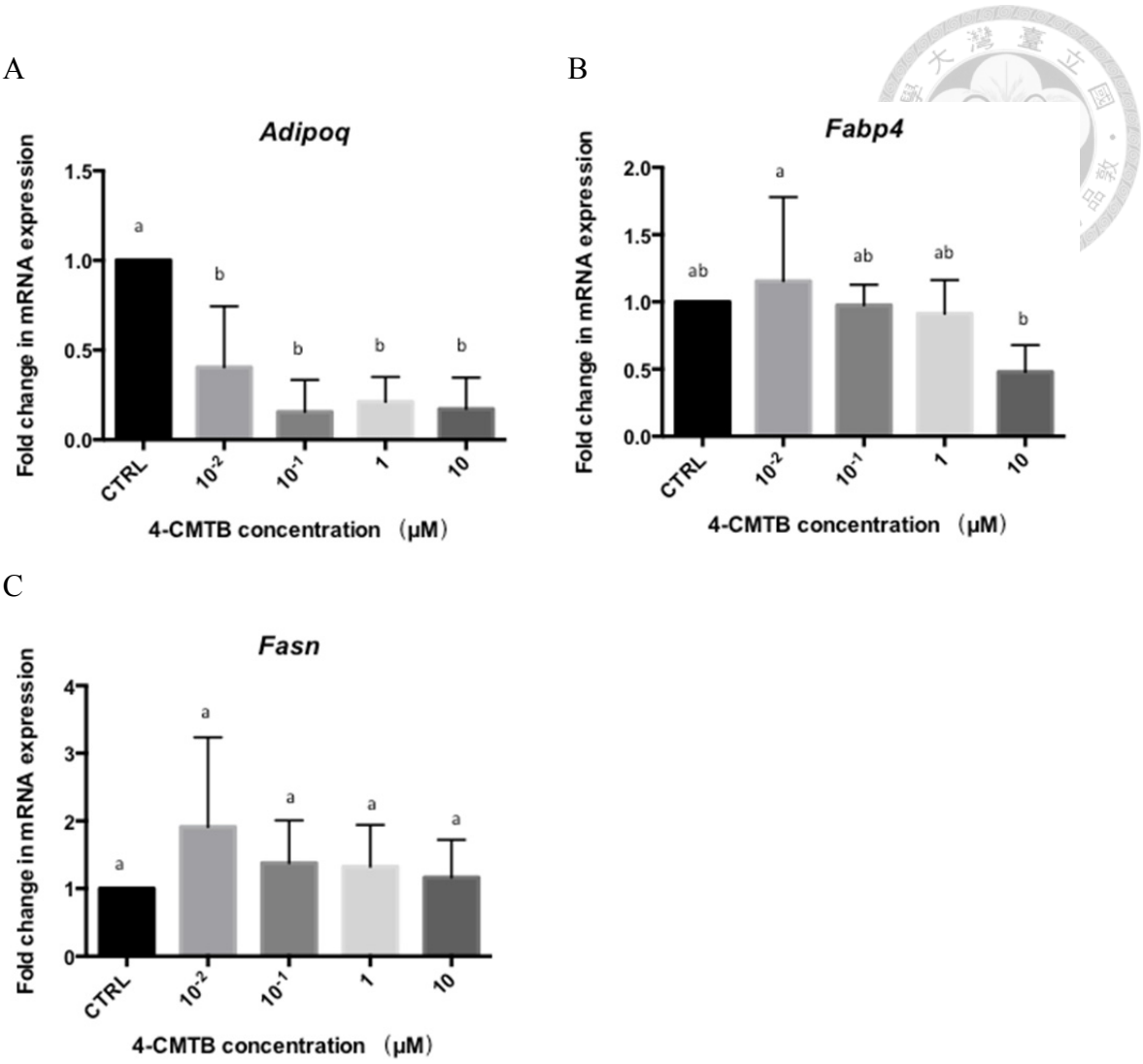

Figure 13. Effects of 4-CMTB on adipogemic markers in mouse SVCs. Mouse SVCs were induced for differentiation in the presence of 0, 10^{-2}, 10^{-1}, 1, or 10 μM 4-CMTB or the vehicle DMSO. Relative mRNA expression of (A) adiponectin (*Adipoq*), (B) fatty acid binding protein 4 (*Fabp4*), and (C) fatty acid synthase (*Fasn*) genes at day 9 were analyzed by real-time qPCR. Data were normalized with 18S mRNA, and presented as means ± SEMs, different letters indicate statistical significance, n = 5, a, b, and c indicate significant difference at $P \leq 0.05$.

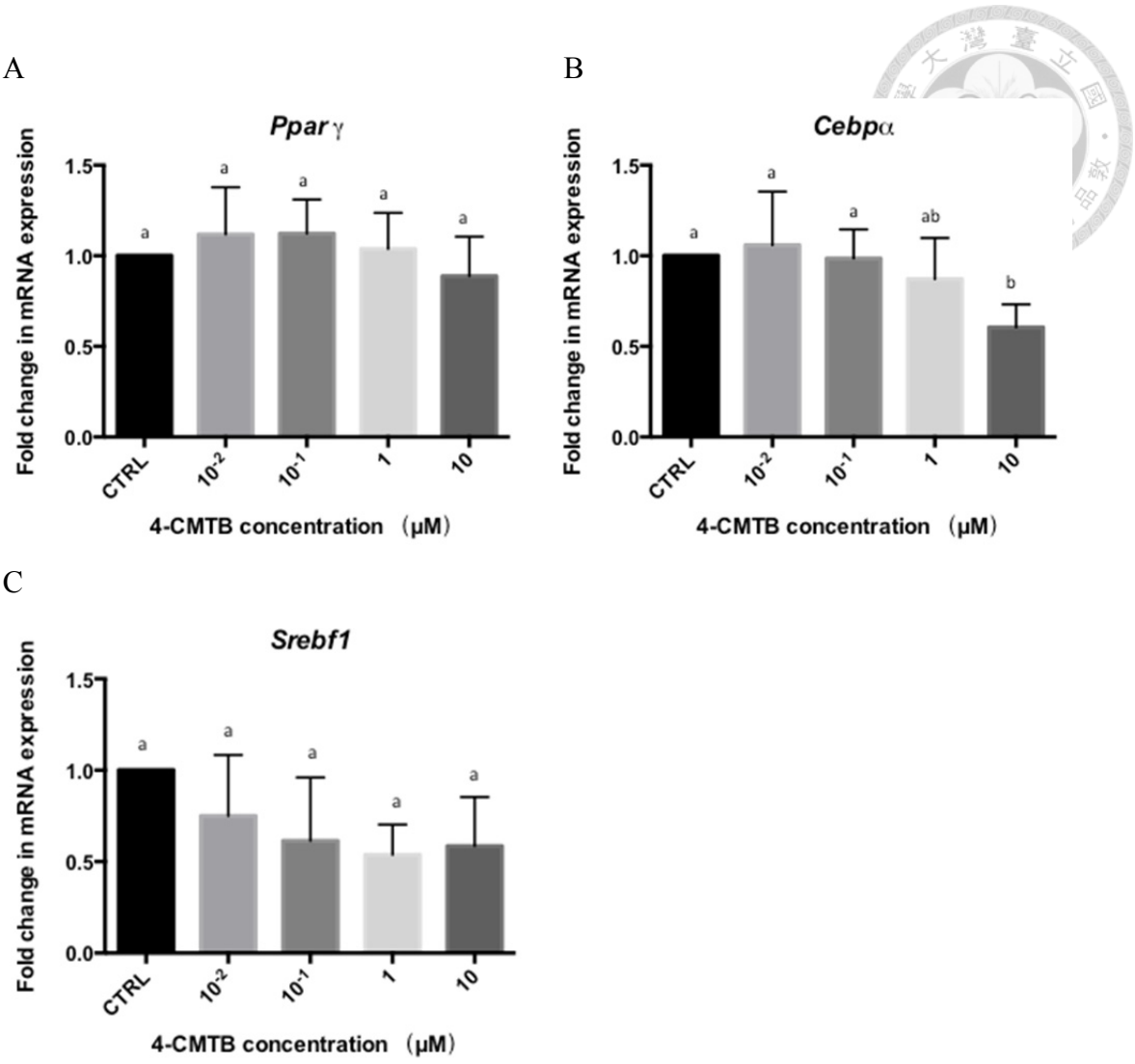

Figure 14. Effects of 4-CMTB on transcription factors in mouse SVCs. Mouse SVCs were induced for differentiation in the presence of 0, 10^{-2}, 10^{-1}, 1, or 10 μM 4-CMTB or the vehicle DMSO. Relative mRNA expression of (A) peroxisome proliferator-activated receptor gamma (*Pparγ*), (B) CCAAT/enhancer-binding protein alpha (*Cebpα*), and (C) sterol regulatory element-binding transcription factor 1 (*SREBF1*) genes at day 9 were analyzed by real-time qPCR. Data were normalized with 18s mRNA, and presented as means ± SEMs, different letters indicate statistical significance, n = 4, a, b, and c indicate significant difference at $P \leq 0.05$.

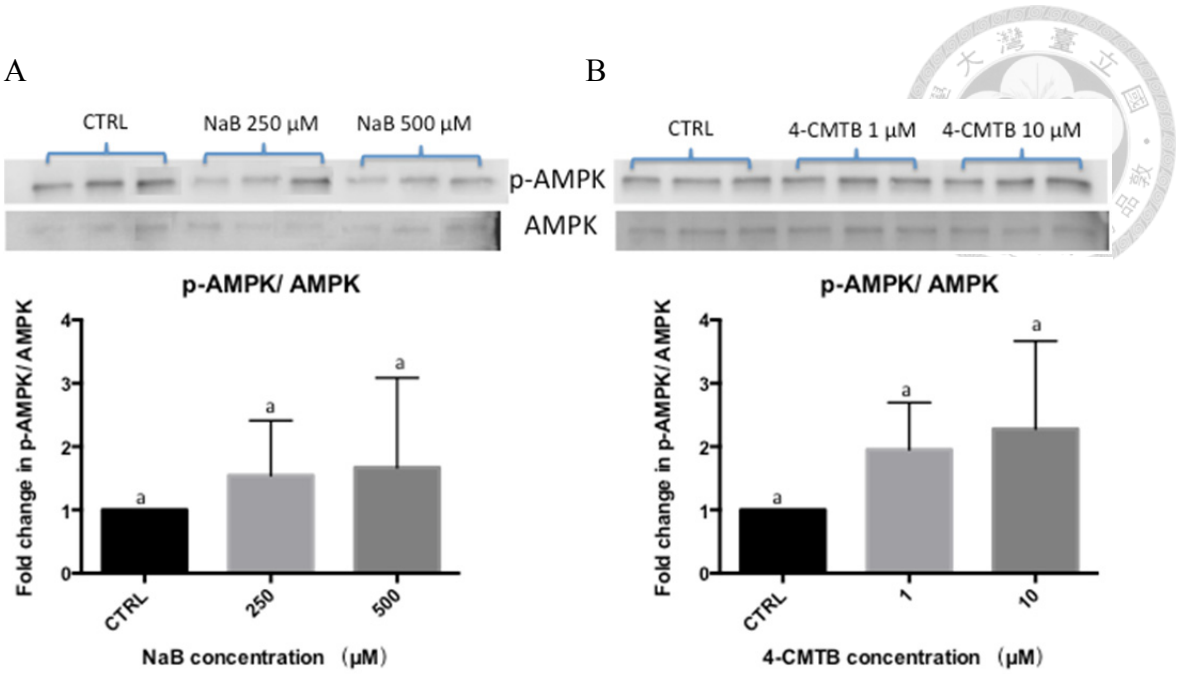

Figure 15. Effects of NaB and 4-CMTB on activation of AMPK in mouse SVCs. Mouse SVCs were induced for differentiation in the presence of 0, 250, or 500 μM NaB (A), and 0, 1, or 10 μM 4-CMTB (B). A representative Western blot analysis and quantification of pAMPK and AMPK ratio in total cellular lysates, presented as means ± SEMs, different letters indicate statistical significance, n = 4, a, b, and c indicate significant difference at $P \leq 0.05$.

4. Discussion

Results of this study are demonstrated distinctive effects and potential mechanism of NaB on adipocyte differentiation in three *in vitro* models, mouse and porcine SVCs, and mouse 3T3-L1 cells. NaB inhibited lipid accumulation of cells (Figure 1) and expression of adipogenic marker *Adipoq*, *Glut4*, *Fabp4*, *Fasn*, *Srebf1* and *Cebpβ* mRNAs (Figure 5; Figure 6C; Figure 7A) differentiating mouse SVCs. Inversely, we also showed that NaB stimulated lipid accumulation in porcine SVCs (Figure 3), with up-regulation of *FASN*, *LPL*, *PPARγ*, *CEBPα*, and *SREBF1* (Figure 10C and D; Figure 11). However, NaB failed to influence adipocyte differentiation in mouse 3T3-L1 cells (Figure 2; Figure 8; Figure 9). These results indicate that NaB effects on adipogenesis depend on species and cell models. NaB induced adipocyte differentiation in porcine SVCs agrees with studies revealing a promotional function of SCFAs in adipocyte differentiation of porcine adipocytes (Li *et al*., 2014). Unexpectedly, NaB showed no obvious effects on adipogenesis of 3T3-L1 cells, it is differ from other studies that SCFAs stimulate 3T3-L1 cells to differentiate into mature adipocytes (Haberland *et al*., 2010; Hong *et al*., 2005; Yoo *et al*., 2006). No effects of SCFAs on adipogenetic program of human SVCs (Chatterjee *et al*., 2011). Nonetheless, NaB was shown to

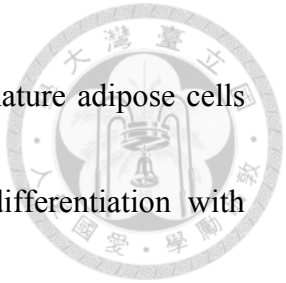

inhibit the differentiation of human mesenchymal stem cells into mature adipose cells (Chen *et al*., 2007). The reasons that SCFAs affect adipocyte differentiation with seemingly incompatible functions are still unknown, but we speculate that these causes may be due to the diverse status among different research groups, such as the use of distinct species, cell models and different experimental operations in cell culture system. On the other hand, we reported the dissimilarity between mouse SVCs primary culture and 3T3-L1 cell line. It is important to point out that even if cells are derived from the same species, different cell types may have distinctive response.

Butyrate is known to bind to FFAR2 and FFAR3 (Bindels *et al*., 2013). In addition, butyrate also have HDAC inhibitory activity (de Ruijter *et al*., 2003). Several prior studies have demonstrated that SCFAs modulate differentiation of pradipocytes by activating FFAR2 or inhibiting HDAC. Hong *et al*. found that the expression amount of *Ffar2* mRNA was high in mouse adipose tissues, but the level of *Ffar3* was not detected. Additionally, *Ffar2* can be detected after differentiating for 3 days in 3T3-L1 cells (Hong *et al*., 2005). Frost and colleagues also exhibited expression of *Ffar2* over 2 days following onset of differentiation in 3T3-L1 cells (Frost *et al*., 2014). Neither *FFAR2* nor *FFAR3* were detected in porcine SVCs before or during adipogenesis (Li *et al*.,

2014). Nonetheless, both HDAC family mRNA or protein expression level can be detected in preadipocytes and mature adipocytes in porcine SVCs, 3T3-L1 cells and other species (Chatterjee *et al*., 2011; Li *et al*., 2014; Yoo *et al*., 2006). Therefore we hypothesized that the discrepant observations of NaB effects may be due to the distinct mechanisms of NaB via different receptor in various species. For example FFAR2 and FFAR3 are not expressed in porcine adipose tissue, they would not have any role in mediating NaB effect in pig. Moreover, FFAR3 mRNA is absent in mouse adipose tissues and undifferentiated or differentiated 3T3-L1 cells. We tested whether 4-CMTB, a specific agonist of FFAR2 which suppresses the mouse SVCs adipogenesis. Mouse SVCs treated with 4-CMTB for 9 days during differentiation showed a remarkable inhibition of lipid droplet accumulation, and low *Adipoq*, *Fabp4*, and *Cebpα* gene expression (Figure 12; Figure 13A and B; Figure 14B). To rule out that the depressing situation is due to the toxicity of drugs used, we initially tested pharmacological dosage, and observed that mouse SVCs cultured with 100 μM for 1 day started to detach from the surface of culture dishes. To avoid this detachment, the highest concentration of 4-CMTB was used as 10 μM, but there was no direct evidence that NaB restrains adipogenic markers expression as well as fat accumulation. These results suggest that

FFAR2 and its agonists function as regulators of adipocyte differentiation in mouse SVCs.

In addition to butyrate, there are lots of compounds affecting adipogenesis. Huang *et al*. suggested that cinnamaldehyde (CA), the major component of cinnamon used in naturopathic medicine, exerts antiadipogenic effects in 3T3-L1 cells (Huang *et al*., 2011). Resveratrol (Res), a natural polyphenolic compound, can inhibit adipocyte differentiation and lipogenesis in 3T3-L1 adipocytes (Chen *et al*., 2011). Other natural products such as dioxinodehydroeckol (DHE), obtained from marine seaweeds also has an effect to inhibit 3T3-L1 pradipocytes differentiation into mature adipocytes (Kim and Kong, 2010). The commonality CA, Res and DHE all diminish adiposity via phosphorylating AMPK. AMPK is a key player in several aspects of energy homeostasis, such as regulating glucose transport, lipolysis or lipogenesis (Daval *et al*., 2006). Furthermore, AMPK is associated with adipogenesis of 3T3-L1 cells, as indicated by the observations that 5-aminoimidazole-4-carboxamide-1-β-D-ribofuranoside (AICAR), a pharmacological activator of AMPK, suppresses expression of adipocyte-specific transcription factors, including Pparγ, Cebpα and Srebf1 (Giri *et al*., 2006; Habinowski and Witters, 2001).

We speculated that NaB and Ffar2 may inhibit adipocyte differentiation in mouse SVCs through AMPK pathway. We found neither NaB treated group nor 4-CMTB treated group showed a significant change of AMPK phosphorylation (Figure 15). These results failed to support our hypothesis that NaB has antiadipogenic effect in mouse SVCs through AMPK.

In conclusion, our results showed that NaB, indeed, plays an important role in regulating adipogenesis. Based on our findings, NaB inhibits the adipocyte differentiation of mouse SVCs, but has no effect on mouse 3T3-L1 cells. However, NaB stimulates the adiposity in porcine SVCs. Furthermore, we also suggested that Ffar2 downregulates the adiposity of mouse SVCs. Although the precise pathways by which NaB induces antiadipogenesis of mouse SVCs remains to be determined, our results might be might be a role of NaB in modifying adipocyte differentiation.

Reference

1. Andoh, A., Y. Fujiyama, K. Hata, Y. Araki, H. Takaya, M. Shimada, and T. Bamba. 1999. Counter-regulatory effect of sodium butyrate on tumour necrosis factor-alpha (TNF-alpha)-induced complement C3 and factor B biosynthesis in human intestinal epithelial cells. Clin. Exp. Immunol. 118:23-9.
2. Aune, U. L., L. Ruiz, and S. Kajimura. 2013. Isolation and differentiation of stromal vascular cells to beige/brite cells. J. Vis. Exp. doi: 10.3791/50191.
3. Bergman, E.N. 1990. Energy contributions of volatile fatty acids from the gastrointestinal tract in various spec. Physiol. Rev. 70:567-90.
4. Bindels, L.B., E. M. Dewulf, and N. M. Delzenne. 2013. GPR43/FFA2: physiopathological relevance and therapeutic prospects. Trends Pharmacol. Sci. 34:226-32.
5. Bjursell, M., T. Admyre, M. Göransson, A. E. Marley, D. M. Smith, J. Oscarsson, and Y. M. Bohlooly. 2011. Improved glucose control and reduced body fat mass in free fatty acid receptor 2-deficient mice fed a high-fat diet. Am. J. Physiol. Endocrinol. Metab. 300:E211-20.
6. Blad, C. C., C. Tang, and S. Offermanns. 2012. G protein-coupled receptors for energy metabolites as new therapeutic targets. Nat. Rev. Drug Discov. 11:603-19.
7. Brahe, L. K., A. Astrup, and L. H. Larsen. 2013. Is butyrate the link between diet, intestinal microbiota and obesity-related metabolic diseases? Obes. Rev. 14:950-9.
8. Brown, A. J., S. M. Goldsworthy, A. A. Barnes, M. M. Eilert, L. Tcheang, D. Daniels, A. I. Muir, M. J. Wigglesworth, I. Kinghorn, N. J. Fraser, N. B. Pike, J. C. Strum, K. M. Steplewski, P. R. Murdock, J. C. Holder, F. H. Marshall, P. G. Szekeres, S. Wilson, D. M. Ignar, S. M. Foord, A. Wise, and S. J. Dowell. 2003. The orphan G protein-coupled receptors GPR41 and GPR43 are activated by propionate and other short chain carboxylic acids. J. Biol. Chem. 278:11312-9.
9. Bugaut, M., and M. Bentéjac. 1993. Biological effects of short-chain fatty acids in nonruminant mammals. Annu. Rev. Nutr. 13:217-41.
10. Burton, G. R., R. Nagarajan, C. A. Peterson, and R. E. McGehee, Jr. 2004. Microarray analysis of differentiation-specific gene expression during 3T3-L1 adipogenesis. Gene 329:167-85.

11. Catalioto, R. M., C. A. Maggi, and S. Giuliani. 2009. Chemically distinct HDAC inhibitors prevent adipose conversion of subcutaneous human white preadipocytes at an early stage of the differentiation program. Exp. Cell Res. 315:3267-80.
12. Chatterjee, T. K., G. Idelman, V. Blanco, A. L. Blomkalns, M. G. Piegore, Jr., D. S. Weintraub, S. Kumar, S. Rajsheker, D. Manka, S. M. Rudich, Y. Tang, D. Y. Hui, R. Bassel-Duby, E. N. Olson, J. B. Lingrel, S. M. Ho, and N. L. Weintraub. 2011. Histone deacetylase 9 is a negative regulator of adipogenic differentiation. J. Biol. Chem. 286:27836-47.
13. Chen, S., Z. Li, W. Li, Z. Shan, and W. Zhu. 2011. Resveratrol inhibits cell differentiation in 3T3-L1 adipocytes via activation of AMPK. Can. J. Physiol. Pharmacol. 89:793-9.
14. Chen, T. H., W. M. Chen, K. H. Hsu, C. D. Kuo, and S. C. Hung. 2007. Sodium butyrate activates ERK to regulate differentiation of mesenchymal stem cells. Biochem Biophys. Res. Commun. 355:913-8.
15. Dagon, Y., Y. Avraham, and E. M. Berry. 2006. AMPK activation regulates apoptosis, adipogenesis, and lipolysis by eIF2alpha in adipocytes. Biochem. Biophys. Res. Commun. 340:43-7.
16. Darlington, G. J., S. E. Ross, and O. A. MacDougald. 1998. The role of C/EBP genes in adipocyte differentiation. J. Biol. Chem. 273:30057-60.
17. Daval, M., F. Foufelle, and P. Ferré. 2006. Functions of AMP-activated protein kinase in adipose tissue. J. Physiol. 574:55-62.
18. Davie, J. R. 2003. Inhibition of histone deacetylase activity by butyrate. J. Nutr. 133:2485S-2493S
19. den Besten, G., K. van Eunen, A. K. Groen, K. Venema, D. J. Reijngoud, B. M. Bakker. 2013. The role of short-chain fatty acids in the interplay between diet, gut microbiota, and host energy metabolism. J. Lipid Res. 54:2325-40.
20. de Ruijter, A. J., A. H. van Gennip, H. N. Caron, S. Kemp, and A. B. van Kuilenburg. 2003. Histone deacetylases (HDACs): characterization of the classical HDAC family. Biochem. J. 370:737-49.
21. Frost, G., Z. Cai, M. Raven, D. T. Otway, R. Mushtaq, and J. D. Johnston. 2014. Effect of short chain fatty acids on the expression of free fatty acid receptor 2 (Ffar2), Ffar3 and early-stage adipogenesis. Nutr. Diabetes 4:e128.

22. Fu, Y., N. Luo, R. L. Klein, and W.T. Garvey. 2005. Adiponectin promotes adipocyte differentiation, insulin sensitivity, and lipid accumulation. J. Lipid Res. 46:1369-79.
23. Gao, L., M. A. Cueto, F. Asselbergs, and P. Atadja. 2002. Cloning and functional characterization of HDAC11, a novel member of the human histone deacetylase family. J. Biol. Chem. 277:25748-55.
24. Gao, Z., J. Yin, J. Zhang, R. E. Ward, R. J. Martin, M. Lefevre, W. T. Cefalu, and J. Ye. 2009. Butyrate improves insulin sensitivity and increases energy expenditure in mice. Diabetes 58:1509-17.
25. Ge, H., X. Li, J. Weiszmann, P. Wang, H. Baribault, J. L. Chen, H. Tian, and Y. Li. 2008. Activation of G protein-coupled receptor 43 in adipocytes leads to inhibition of lipolysis and suppression of plasma free fatty acids. Endocrinology 149:4519-26.
26. Giri, S., R. Rattan, E. Haq, M. Khan, R. Yasmin, J. S. Won, L. Key, A. K. Singh, and I. Singh. 2006. AICAR inhibits adipocyte differentiation in 3T3L1 and restores metabolic alterations in diet-induced obesity mice model. Nutr. Metab. (Lond) 3:31.
27. Haberland, M., M. Carrer, M. H. Mokalled, R. L. Montgomery, and E. N. Olson. 2010. Redundant control of adipogenesis by histone deacetylases 1 and 2. J. Biol. Chem. 285:14663-70.
28. Habinowski, S. A., and L. A. Witters. 2001. The effects of AICAR on adipocyte differentiation of 3T3-L1 cells. Biochem. Biophys. Res. Commun. 286:852-6.
29. Hamer, H. M., D. Jonkers, K. Venema, S. Vanhoutvin, F. J. Troost, and R. J. Brummer. 2008. Review article: the role of butyrate on colonic function. Aliment. Pharmacol. Ther. 27:104-19.
30. Haumaitre, C., O. Lenoir, and R. Scharfmann. 2008. Histone deacetylase inhibitors modify pancreatic cell fate determination and amplify endocrine progenitors. Mol. Cell Biol. 28:6373-83.
31. Henkens, T., P. Papeleu, G. Elaut, M. Vinken, V. Rogiers, and T. Vanhaecke. 2007. Trichostatin A, a critical factor in maintaining the functional differentiation of primary cultured rat hepatocytes. Toxicol. Appl. Pharmacol. 218:64-71.
32. Hong, Y. H., Y. Nishimura, D. Hishikawa, H. Tsuzuki, H. Miyahara, C. Gotoh, K. C. Choi, D. D. Feng, C. Chen, H. G. Lee, K. Katoh, S. D. Roh, and S. Sasaki. 2005. Acetate and propionate short chain fatty acids stimulate adipogenesis via GPCR43. Endocrinology 146:5092-9.

33. Huang, B., H. D. Yuan, D. Y. Kim, H. Y. Quan, and S. H. Chung. 2011. Cinnamaldehyde prevents adipocyte differentiation and adipogenesis via regulation of peroxisome proliferator-activated receptor-gamma (PPARgamma) and AMP-activated protein kinase (AMPK) pathways. J. Agric. Food Chem. 59:3666-73.
34. Jacobs, M. D., and S. C. Harrison. 1998. Structure of an IkappaBalpha/NF-kappaB complex. Cell 95:749-58.
35. Kashihara, K. Hirano, T. Tani, T. Takahashi, S. Miyauchi, G. Shioi, H. Inoue, and G. Tsujimoto. 2013. The gut microbiota suppresses insulin-mediated fat accumulation via the short-chain fatty acid receptor GPR43. Nat. Commun. 4:1829.
36. Kim, M. H., S. G. Kang, J. H. Park, M. Yanagisawa, and C. H. Kim. 2013. Short-chain fatty acids activate GPR41 and GPR43 on intestinal epithelial cells to promote inflammatory responses in mice. Gastroenterology 145:396-406.
37. Kim, S. K., and C. S. Kong. 2010. Anti-adipogenic effect of dioxinodehydroeckol via AMPK activation in 3T3-L1 adipocytes. Chem. Biol. Interact. 186:24-9.
38. Kim, S. N., H. Y. Choi, and Y. K. Kim. 2009. Regulation of adipocyte differentiation by histone deacetylase inhibitors. Arch. Pharm. Res. 32:535-41.
39. Kimura, I., K. Ozawa, D. Inoue, T. Imamura, K. Kimura, T. Maeda, K. Terasawa, D. Kashihara, K. Hirano, T. Tani, T. Takahashi, S. Miyauchi, G. Shioi, H. Inoue, and G. Tsujimoto. 2013. The gut microbiota suppresses insulin-mediated fat accumulation via the short-chain fatty acid receptor GPR43. Nat. Commun. 4:1829.
40. Lagace, D. C., and M. W. Nachtigal. 2004. Inhibition of histone deacetylase activity by valproic acid blocks adipogenesis. J. Biol. Chem. 279:18851-60.
41. Le Poul, E., C. Loison, S. Struyf, J. Y. Springael, V. Lannoy, M. E. Decobecq, S. Brezillon, V. Dupriez, G. Vassart, J. Van Damme, M. Parmentier, and M. Detheux. 2003. Functional characterization of human receptors for short chain fatty acids and their role in polymorphonuclear cell activation. J. Biol. Chem. 278:25481-9.
42. Li, G., H. Su, Z. Zhou, and W. Yao. 2014. Identification of the porcine G protein-coupled receptor 41 and 43 genes and their expression pattern in different tissues and development stages. PLoS One 9:e97342.
43. Li, G., W. Yao, and H. Jiang. 2014. Short-chain fatty acids enhance adipocyte differentiation in the stromal vascular fraction of porcine adipose tissue. J. Nutr. 144:1887-95.

44. Li, H., L. Myeroff, D. Smiraglia, M. F. Romero, T. P. Pretlow, L. Kasturi, J. Lutterbaugh, R. M. Rerko, G. Casey, J. P. Issa, J. Willis, J. K. Willson, C. Plass, and S. D. Markowitz. 2003. SLC5A8, a sodium transporter, is a tumor suppressor gene silenced by methylation in human colon aberrant crypt foci and cancers. Proc. Natl. Acad. Sci. U. S. A. 100:8412-7.
45. Li, H. P., X. Chen, and M. Q. Li. 2013. Butyrate alleviates metabolic impairments and protects pancreatic beta cell function in pregnant mice with obesity. Int. J. Clin. Exp. Pathol. 6:1574-84.
46. Liu, B. H., Y. C. Wang, C. F. Kuo, W. M. Cheng, T. F. Shen, and S. T. Ding. 2005. The effects of docosahexaenoic acid oil and soybean oil on the expression of lipid metabolism related mrna in pigs. J. Anim. Sci. 18:1451-1456.
47. Liu, L. R., S. P. Lin, C. C. Chen, Y. J. Chen, C. C. Tai, S. C. Chang, R. H. Juang, Y. W. Tseng, B. H. Liu, H. J. Mersmann, T. L. Shen, and S. T. Ding. 2011. Serum amyloid A induces lipolysis by downregulating perilipin through ERK1/2 and PKA signaling pathways. Obesity (Silver Spring) 19:2301-9.
48. McKinsey, T. A., C. L. Zhang, and E. N. Olson. 2001. Control of muscle development by dueling HATs and HDACs. Curr. Opin. Genet. Dev. 11:497-504.
49. Milligan, G., L. A. Stoddart, and N. J. Smith. 2009. Agonism and allosterism: the pharmacology of the free fatty acid receptors FFA2 and FFA3. Br. J. Pharmacol. 158:146-53.
50. Ntambi, J. M., and Y. C. Kim. 2000. Adipocyte differentiation and gene expression. J. Nutr. 130:3122S-3126S.
51. Payne, V. A., W. S. Au, C. E. Lowe, S. M. Rahman, J. E. Friedman, S. O'Rahilly, and J. J. Rochford. 2010. C/EBP transcription factors regulate SREBP1c gene expression during adipogenesis. Biochem. J. 425:215-23.
52. Pfaffl, M.W. 2001. A new mathematical model for relative quantification in real-time RT-PCR. Nucleic Acids Res. 29:e45.
53. Pryde, S. E., S. H. Duncan, G. L. Hold, C. S. Stewart, and H. J. Flint. 2002. The microbiology of butyrate formation in the human colon. FEMS Microbiol. Lett. 217:133-9.
54. Rahman, M. M., A. Kukita, T. Kukita, T. Shobuike, T. Nakamura, and O. Kohashi. 2003. Two histone deacetylase inhibitors, trichostatin A and sodium butyrate, suppress differentiation into osteoclasts but not into macrophages. Blood 101:3451-9.

55. Rosen, E. D., and O. A. MacDougald. 2006. Adipocyte differentiation from the inside out. Nat. Rev. Mol. Cell Biol. 7:885-96.
56. Smith, N. J., R. J. Ward, L. A. Stoddart, B. D. Hudson, E. Kostenis, T. Ulven, J. C. Morris, C. Tränkle, I. G. Tikhonova, D. R. Adams, and G. Milligan. 2011. Extracellular loop 2 of the free fatty acid receptor 2 mediates allosterism of a phenylacetamide ago-allosteric modulator. Mol. Pharmacol. 80:163-73.
57. Spiegelman, B. M., E. Hu, J. B. Kim, and R. Brun. 1997. PPARgamma and the control of adipogenesis. Biochimie. 79:111-2.
58. Symonds, M. E. Adipose Tissue Biology. New York: Springer-Verlag, 2012, ch.2.
59. Talukdar, S., J. M. Olefsky, and O. Osborn. 2011. Targeting GPR120 and other fatty acid-sensing GPCRs ameliorates insulin resistance and inflammatory diseases. Trends. Pharmacol. Sci. 32:543-50.
60. Tang, C., K. Ahmed, A. Gille, S. Lu, H. J. Gröne, S. Tunaru, and S. Offermanns. 2015. Loss of FFA2 and FFA3 increases insulin secretion and improves glucose tolerance in type 2 diabetes. Nat. Med. 21:173-7.
61. Tazoe, H., Y. Otomo, I. Kaji, R. Tanaka, S. I. Karaki, and A. Kuwahara. 2008. Roles of short-chain fatty acids receptors, GPR41 and GPR43 on colonic functions. J. Physiol. Pharmacol. 59 Suppl 2:251-62.
62. Tou, L., Q. Liu, and R. A. Shivdasani. 2004. Regulation of mammalian epithelial differentiation and intestine development by class I histone deacetylases. Mol. Cell Biol. 24:3132-9.
63. Trompette, A., E. S. Gollwitzer, K. Yadava, A. K. Sichelstiel, N. Sprenger, C. Ngom-Bru, C. Blanchard, T. Junt, L. P. Nicod, N. L. Harris, and B. J. Marsland. 2014. Gut microbiota metabolism of dietary fiber influences allergic airway disease and hematopoiesis. Nat. Med. 20:159-66.
64. Trzaskowski, B., D. Latek, S. Yuan, U. Ghoshdastider, A. Debinski, and S. Filipek. 2012. Action of molecular switches in GPCRs-theoretical and experimental studies. Curr. Med. Chem. 19:1090-109.
65. Ulven, T. 2012. Short-chain free fatty acid receptors FFA2/GPR43 and FFA3/GPR41 as new potential therapeutic targets. Front. Endocrinol. (Lausanne). 3:111.
66. Unger, R. H., G. O. Clark, P. E. Scherer, and L. Orci. 2010. Lipid homeostasis, lipotoxicity and the metabolic syndrome. Biochim. Biophys. Acta. 1801:209-14.

67. Vinolo, M. A., H. G. Rodrigues, R. T. Nachbar, and R. Curi. 2011. Regulation of inflammation by short chain fatty acids. Nutrients 3:858-76.
68. Wang, J., X. Wu, N. Simonavicius, H. Tian, and L. Ling. 2006. Medium-chain fatty acids as ligands for orphan G protein-coupled receptor GPR84. J. Biol. Chem. 281:34457-64.
69. Wang, M. Y., P. Grayburn, S. Chen, M. Ravazzola, L. Orci, and R. H. Unger. 2008. Adipogenic capacity and the susceptibility to type 2 diabetes and metabolic syndrome. Proc. Natl. Acad. Sci. U. S. A. 105:6139-44.
70. Xiong, Y., N. Miyamoto, K. Shibata, M. A. Valasek, T. Motoike, R. M. Kedzierski, and M. Yanagisawa. 2004. Short-chain fatty acids stimulate leptin production in adipocytes through the G protein-coupled receptor GPR41. Proc. Natl. Acad. Sci. U. S. A. 101:1045-50.
71. Xu, W. S., R. B. Parmigiani, and P. A. Marks. 2007. Histone deacetylase inhibitors: molecular mechanisms of action. Oncogene 26:5541-52.
72. Yang, J., Y. Kawai, R. W. Hanson, and I. J. Arinze. 2001. Sodium butyrate induces transcription from the G alpha(i2) gene promoter through multiple Sp1 sites in the promoter and by activating the MEK-ERK signal transduction pathway. J. Biol. Chem. 276:25742-52.
73. Yin, L., G. Laevsky, and C. Giardina. 2001. Butyrate suppression of colonocyte NF-kappa B activation and cellular proteasome activity. J. Biol. Chem. 276:44641-6.
74. Yonezawa, T., R. Kurata, K. Yoshida, M. A. Murayama, X. Cui, and A. Hasegawa. 2013. Free fatty acids-sensing G protein-coupled receptors in drug targeting and therapeutics. Curr. Med. Chem. 20:3855-71.
75. Yoo, E. J., J. J. Chung, S. S. Choe, K. H. Kim, and J. B. Kim. 2006. Down-regulation of histone deacetylases stimulates adipocyte differentiation. J. Biol. Chem. 281:6608-15.
76. Zaibi, M. S., C. J. Stocker, J. O'Dowd, A. Davies, M. Bellahcene, M. A. Cawthorne, A. J. Brown, D. M. Smith, and J. R. Arch. 2010. Roles of GPR41 and GPR43 in leptin secretory responses of murine adipocytes to short chain fatty acids. FEBS Lett. 584:2381-6.